

CERN-EP-2017-107
2017/11/22

CMS-B2G-16-024

Search for pair production of vector-like T and B quarks in single-lepton final states using boosted jet substructure in proton-proton collisions at $\sqrt{s} = 13$ TeV

The CMS Collaboration*

Abstract

A search for pair production of massive vector-like T and B quarks in proton-proton collisions at $\sqrt{s} = 13$ TeV is presented. The data set was collected in 2015 by the CMS experiment at the LHC and corresponds to an integrated luminosity of up to 2.6 fb^{-1} . The T and B quarks are assumed to decay through three possible channels into a heavy boson (either a W, Z or Higgs boson) and a third generation quark. This search is performed in final states with one charged lepton and several jets, exploiting techniques to identify W or Higgs bosons decaying hadronically with large transverse momenta. No excess over the predicted standard model background is observed. Upper limits at 95% confidence level on the T quark pair production cross section are set that exclude T quark masses below 860 GeV in the singlet, and below 830 GeV in the doublet branching fraction scenario. For other branching fraction combinations with $\mathcal{B}(T \rightarrow tH) + \mathcal{B}(T \rightarrow bW) \geq 0.4$, lower limits on the T quark range from 790 to 940 GeV. Limits are also set on pair production of singlet vector-like B quarks, which can be excluded up to a mass of 730 GeV. The techniques showcased here for understanding highly-boosted final states are important as the sensitivity to new particles is extended to higher masses.

Published in the Journal of High Energy Physics as doi:10.1007/JHEP11(2017)085.

1 Introduction

The discovery of a light mass Higgs boson (H) [1–3] motivates searches for new interactions and particles at the LHC [4]. Cancellation of the loop corrections to the Higgs boson mass without precise fine tuning of parameters requires new particles at the TeV scale. Such new particles are the bosonic partners of the top quark, in supersymmetric models, or the fermionic top quark partners predicted by many other theories, such as little Higgs [5, 6] and composite Higgs [7–10] models. These heavy quark partners predominantly mix with the third-generation quarks of the standard model (SM) [11, 12] and have vector-like transformation properties under the SM gauge group $SU(2)_L \times U(1)_Y \times SU(3)_C$, hence the term “vector-like quarks” (VLQ). While a chiral extension of the SM quark family has been strongly disfavored by precision electroweak studies at electron-positron colliders [13, 14] and by observed production cross sections and branching fractions of the Higgs boson [15], models with VLQs are not excluded by present data.

We search for a vector-like T quark with charge $2/3$ (in units of the electron charge) that is produced via the strong interaction in proton-proton collisions along with its antiquark, \bar{T} . Many models in which VLQs appear assume that T quarks decay to three final states: bW , tZ , or tH [16]. Leading-order Feynman diagrams of these three processes are shown in Fig. 1, created with the tools of Ref. [17]. The partial decay widths depend on the particular model [18], so that the branching fractions of these decay modes can take on various possible values, with the sum of all three branching fractions equal to unity. An electroweak isospin singlet T quark is expected to have a branching fraction of approximately 50% for $T \rightarrow bW$, and 25% for each of $T \rightarrow tZ$ and tH , and is used as a benchmark for figures and tables. A T quark in a weak isospin doublet has no decays to bW and equal branching fractions for tZ and tH decays [18–20]. As these are, however, not the only possible representations of T quarks, the final results are interpreted for many allowed branching fraction combinations.

Though this search is optimized for $T\bar{T}$ production, decays of vector-like bottom quark partners (B quarks) can produce similar topologies and $B\bar{B}$ production is also considered. The B quark with charge $-1/3$ is expected to decay to tW , bH , or bZ and can also transform either as a singlet or doublet under the electroweak symmetry group. The respective branching fractions are equal to those of the corresponding T quark decays to the same SM bosons. For this search we assume that only one new particle is present, either the T or B quark.

Most recently, searches for pair-produced T and B quarks were performed by both the ATLAS and CMS collaborations at $\sqrt{s} = 8$ TeV [21–26]. Depending on the assumed combination of branching fractions to the three decay modes, the CMS collaboration observed lower limits on the T quark mass with values ranging from 720 to 920 GeV and on the B quark mass with values ranging from 740 to 900 GeV at 95% confidence level (CL) [21, 25]. The ATLAS collaboration found similar lower mass limits, so that vector-like T and B quarks with masses below 720 GeV

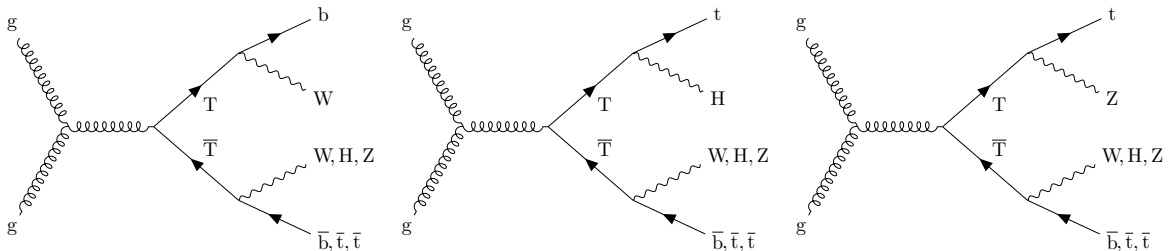


Figure 1: Examples of leading-order Feynman diagrams showing production of a $T\bar{T}$ pair with the T quark decaying to bW (left), tH (middle), and tZ (right).

are already excluded for all possible branching fraction combinations. We therefore only consider VLQ masses above 700 GeV in this search. The ATLAS collaboration has also searched for pair production of T and B quarks at $\sqrt{s} = 13$ TeV [27, 28].

We require one electron or one muon in the final state, along with several jets. All decay modes of the T and B quarks produce t quarks and/or W bosons, which are the dominant sources of leptons. In the high mass region that we consider, the decay products can have a large Lorentz boost and result in highly collinear final state particles. This search makes use of techniques to identify b quark jets and reconstruct hadronic decays of massive particles that are highly Lorentz-boosted in the reference frame of the $T\bar{T}$ system. The data are analyzed in two channels that are optimized for sensitivity to either boosted W or Higgs bosons, referred to as the “boosted W” and “boosted H” channels. The boosted W channel is most sensitive to scenarios where the T quark has a large branching fraction for bW decays (such as the electroweak singlet benchmark) while the boosted H channel has the highest sensitivity to scenarios with a large branching fraction to tH (such as the electroweak doublet benchmark). The $T \rightarrow tZ$ decay mode is not a particular target of this search, but Lorentz-boosted Z bosons decaying hadronically can be selected in either channel since the signatures are similar to those of boosted hadronic W or Higgs boson decays, thus providing some sensitivity to the tZ decay mode.

2 The CMS detector and event reconstruction

The central feature of the CMS apparatus is a superconducting solenoid of 6 m internal diameter, providing a magnetic field of 3.8 T. Within the solenoid volume are a silicon pixel and strip tracker, a lead tungstate crystal electromagnetic calorimeter (ECAL), and a brass and scintillator hadron calorimeter (HCAL), each composed of a barrel and two endcap sections. Forward calorimeters extend the pseudorapidity (η) [29] coverage provided by the barrel and endcap detectors. Muons are measured in gas-ionization detectors embedded in the steel flux-return yoke outside the solenoid.

A particle-flow (PF) algorithm [30] is used to reconstruct and identify each individual particle in an event with an optimized combination of information from the various elements of the CMS detector. The energy of photons is directly obtained from the ECAL measurement, corrected for zero-suppression effects. The energy of electrons is determined from a combination of the electron momentum at the primary interaction vertex as determined by the tracker, the energy of the corresponding ECAL cluster, and the energy sum of all bremsstrahlung photons spatially compatible with originating from the electron track. The momentum resolution for electrons with transverse momentum $p_T \approx 45$ GeV from $Z \rightarrow e^+e^-$ decays ranges from 1.7% for low-bremsstrahlung electrons in the barrel region to 4.5% for showering electrons in the endcaps [31]. The energy of muons is obtained from the curvature of the corresponding track. Matching muons to tracks measured in the silicon tracker results in a relative transverse momentum resolution for muons with $20 < p_T < 100$ GeV of 1.3–2.0% in the barrel and better than 6% in the endcaps. The p_T resolution in the barrel is better than 10% for muons with p_T up to 1 TeV [32]. The energy of charged hadrons is determined from a combination of their momenta measured in the tracker and the matching ECAL and HCAL energy deposits, corrected for zero-suppression effects and for the response function of the calorimeters to hadronic showers. Finally, the energy of neutral hadrons is obtained from the corresponding corrected ECAL and HCAL energy.

Jets are reconstructed from the individual particles produced by the PF event algorithm, clustered using the anti- k_T algorithm [33, 34] with distance parameters of 0.4 (“AK4 jets”) or 0.8 (“AK8 jets”). Jet momentum is defined as the vectorial sum of all particle momenta in the jet,

and is found from simulation to be within 5 to 10% of the true momentum over the whole p_T spectrum and detector acceptance. All jets are required to have $|\eta| < 2.5$ and AK4 (AK8) jets must have $p_T > 30$ (200) GeV. An offset correction is applied to jet energies to take into account the contribution from additional proton-proton interactions within the same or nearby bunch crossings (pileup) [35]. Jet energy corrections are derived from simulation, and are confirmed with in situ measurements of the energy balance in dijet and photon/Z($\rightarrow ee/\mu\mu$) + jet events [36]. A smearing of the jet energy is applied to simulated events to mimic the energy resolution observed in data, typically 15% at 10 GeV, 8% at 100 GeV, and 4% at 1 TeV. Additional selection criteria are applied to each event to remove spurious jet-like features originating from isolated noise patterns in the HCAL [37], anomalously high energy deposits in certain regions of the ECAL, and cosmic ray and beam halo particles that are detected in the muon chambers.

The missing transverse momentum vector is defined as the projection on the plane perpendicular to the beams of the negative vector sum of the momenta of all reconstructed particles in an event. Its magnitude is referred to as E_T^{miss} . The energy scale corrections applied to jets are propagated to E_T^{miss} .

A more detailed description of the CMS detector, together with a definition of the coordinate system used and the relevant kinematic variables, can be found in Ref. [29].

3 Data and simulated samples

The data used in this analysis were collected during 2015 when the LHC collided protons at $\sqrt{s} = 13$ TeV with a bunch spacing of 25 ns. The data set for the boosted W channel corresponds to an integrated luminosity of 2.3 fb^{-1} . The data set for the boosted H channel in the electron (muon) channel corresponds to 2.5 (2.6) fb^{-1} and includes additional data collected with poor forward calorimeter performance where the E_T^{miss} has been re-computed excluding the affected region of the detector.

To compare the SM expectation with the experimental data, samples of events for all relevant SM background processes and the $T\bar{T}$ signal are produced using Monte Carlo (MC) simulation. Background processes are simulated using several matrix element generators. The POWHEG v2 generator [38–41] is used to simulate $t\bar{t}$ events, as well as single top quark events in the tW channel at next-to-leading order (NLO). The MADGRAPH5.aMC@NLO 2.2.2 generator [42] is used for generation at NLO of Drell–Yan + jets and $t\bar{t} + W$ events, as well as $t\bar{t} + Z$ events, and s - and t -channel production of single top quarks. The FxFx scheme [43] for merging matrix element generation to the parton shower is used. The MADGRAPH v5.2.2.2 generator is used with the MLM scheme [44] to generate W + jets, Drell–Yan + jets, and multijet events at leading order. PYTHIA 8.212 [45, 46] is used for the simulation of multijet and diboson events.

The boosted W channel uses the NLO Drell–Yan + jets simulation and the MADGRAPH multijet simulation. The boosted H channel uses the MADGRAPH Drell–Yan + jets simulation, and the PYTHIA multijet simulation which is filtered for processes likely to pass the lepton selection in this channel. Background samples are grouped into three categories for presentation: “TOP”, dominated by $t\bar{t}$ and including single top quark and $t\bar{t} + W/Z$ samples; “EW”, dominated by W + jets and including Drell–Yan + jets and diboson samples; and “QCD”, including multijet samples.

Signal samples for both $T\bar{T}$ and $B\bar{B}$ production are simulated using MADGRAPH for mass points between 700 and 1800 GeV in steps of 100 GeV. A narrow width of 10 GeV is assumed for the vector-like quarks. Predicted cross sections, which depend only on the vector-like quark mass,

Table 1: Predicted cross sections for pair production of T or B quarks for various masses. Uncertainties include contributions from energy scale variations and from the PDFs.

T or B quark mass [GeV]	Cross section [fb]
700	455 ± 19
800	196 ± 8
900	90 ± 4
1000	44 ± 2
1100	22 ± 1
1200	11.8 ± 0.6
1300	$6.4 \pm^{0.4}_{0.3}$
1400	3.5 ± 0.2
1500	2.0 ± 0.1
1600	$1.15 \pm^{0.09}_{0.07}$
1700	$0.67 \pm^{0.06}_{0.04}$
1800	$0.39 \pm^{0.04}_{0.03}$

are computed at next-to-next-to-leading order (NNLO) with the TOP++2.0 program [47–52] and are listed in Table 1.

Parton showering and the underlying event for all simulated samples are obtained with PYTHIA using the CUETP8M1 tune [53, 54]. To simulate the momentum spectrum of partons inside the colliding protons, the NNPDF3.0 [55] parton distribution functions (PDFs) are used. Detector simulation for all MC samples is performed with GEANT4 [56] and includes the effect of pileup.

4 Reconstruction methods

We perform a search for T quarks that decay to final states with an electron or a muon, and jets. Selected events must have one or more pp interaction vertices within the luminous region (longitudinal position $|z| < 24$ cm and radial position $\rho < 2$ cm), reconstructed using a deterministic annealing filter algorithm [57]. The primary interaction vertex is the vertex with the largest $\sum p_T^2$ from its associated jets, leptons, and E_T^{miss} . The number of pileup interactions differs between data and simulation, so simulated events are weighted to reflect the pileup distribution expected in data given a total inelastic cross section of 69 mb [58].

Two observables that are useful in discriminating signal from background events, exploiting the fact that the decays of T quarks to single-lepton final states produce a large number of hadronic objects, are the following: the quantity H_T , defined as the scalar p_T sum of all reconstructed AK4 jets with $p_T > 30$ GeV and $|\eta| < 2.4$, and the quantity S_T , defined as the scalar sum of E_T^{miss} , the p_T of the lepton, and H_T .

4.1 Lepton reconstruction and selection

This search requires one charged lepton, either an electron or a muon, to be reconstructed within the acceptance region of $|\eta| < 2.4$. The event must satisfy a single-electron or single-muon trigger. The choice of triggers is adapted to the particular final state targeted in each channel. In $T \rightarrow bW$ decays, the W boson is generally well separated from the associated bottom quark since the T quark has low p_T compared to its mass, leading to a low level of hadronic activity in close proximity to the lepton. In contrast, a lepton originating from a top

quark decay (e.g., from a $T \rightarrow tH$ decay) becomes increasingly collinear with the associated bottom quark as the T quark mass increases and the Lorentz boost of the top quark rises.

As a consequence of the above, the boosted W channel uses triggers selecting leptons that are isolated with respect to nearby PF candidates, either electron candidates with $p_T > 27$ GeV and $|\eta| < 2.1$, or muon candidates with $p_T > 20$ GeV. The triggers used in the boosted H channel do not require that the leptons are isolated. In the electron channel, events with at least one electron candidate with $p_T > 45$ GeV, one AK4 jet with $p_T > 200$ GeV, and another AK4 jet with $p_T > 50$ GeV are selected by the trigger. The muon channel trigger selects events with a muon candidate with $p_T > 45$ GeV and $|\eta| < 2.1$. Methods to evaluate lepton isolation efficiency after trigger selection are described below.

Additional lepton identification quality criteria are required to reduce the contribution from background events containing other particles misidentified as leptons. For electrons these quality requirements [31] combine variables measuring track quality, the association between the track and electromagnetic shower, shower shape, and the likelihood of the electron to originate from a photon. Electrons are identified in the boosted H channel using a set of selection criteria with an efficiency of $\approx 88\%$ and misidentification rate of $\approx 7\%$. In the boosted W channel, two working points are defined based on a multivariate identification algorithm: a tight level with $\approx 88\%$ efficiency ($\approx 4\%$ misidentification rate) and a loose level with $\approx 95\%$ efficiency ($\approx 5\%$ misidentification rate).

Muons are reconstructed by fitting hits in the silicon tracker together with hits in the muon detectors [32]. Identification algorithms consider the quality of this fit, the number or fraction of valid hits in the trackers and muon detectors, track kinks, and the minimum distance between the extrapolated track from the silicon tracker and the primary interaction vertex. Several working points are defined: the boosted W channel uses so-called “tight” (“loose”) muons with $\approx 97\%$ (100%) efficiency in the barrel region, and the boosted H channel uses “medium” muons with $\approx 99\%$ efficiency in the barrel region. All muon identification working points have hadron misidentification rates of $< 1\%$.

Leptons that pass the requirements in the two channels are removed from jets that have an angular separation of $\Delta R < 0.4$ from the lepton. This is done by matching PF candidates identified as leptons to the ones identified as jets and subtracting the four-momentum of a matched lepton candidate from the jet four-momentum.

In order to reduce the rate of background events that contain a soft lepton (e.g., from semileptonic bottom quark decays in multijet events), several metrics can be used to evaluate the isolation of a lepton from surrounding particles. In the boosted H channel, either an angular separation of $\Delta R(\ell, j) > 0.4$, or $p_T^{\text{rel}}(\ell, j) > 40$ GeV is required. Here, ℓ denotes the highest p_T lepton, j is the jet closest to that lepton in angular separation, and $p_T^{\text{rel}}(\ell, j)$ is the projection of the lepton momentum on the direction perpendicular to the jet momentum in the ℓ - j plane. These criteria, also referred to as “2D isolation”, ensure a high signal efficiency for decays such as $T \rightarrow tH$, with leptons produced close to jets, while rejecting a large fraction of the multijet background.

In the boosted W channel, where fewer leptons with nearby b quarks are expected, isolation is evaluated using mini-isolation (I_{mini}), defined as the sum of the transverse momenta of PF candidates within a p_T -dependent cone around the lepton, corrected for the effects of pileup and divided by the lepton p_T . The radius of the isolation cone, R_I , is defined as:

$$R_I = \frac{10 \text{ GeV}}{\min(\max(p_T, 50 \text{ GeV}), 200 \text{ GeV})}. \quad (1)$$

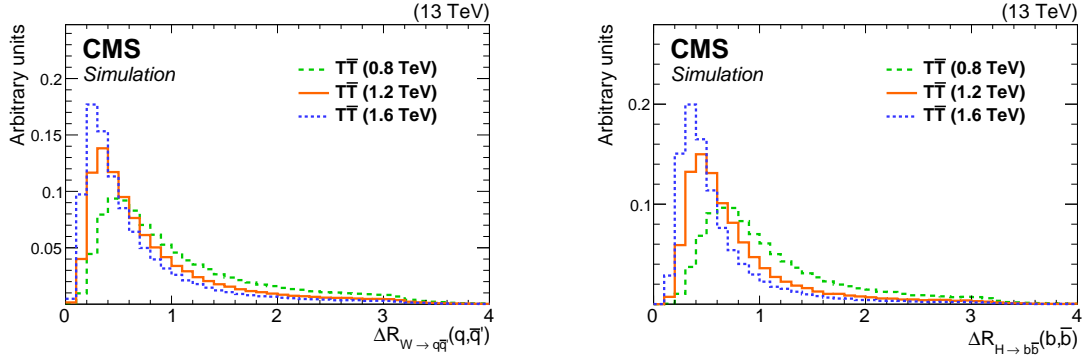


Figure 2: Angular separations ΔR between the products of simulated $W \rightarrow q\bar{q}'$ (left) and $H \rightarrow b\bar{b}$ (right) decay processes for three different mass points of the T quark. Even for the lowest mass point shown, the final state particles are typically emitted with a separation of $\Delta R < 0.8$ and are merged into an AK8 jet.

Using a p_T -dependent cone size allows for greater efficiency at high energies where jets and leptons are more likely to overlap. “Tight” electrons (muons) must have $I_{\text{mini}} < 0.1$ (0.2) while “loose” electrons and muons satisfy $I_{\text{mini}} < 0.4$. In addition, the 2D isolation requirement is applied to remove any residual overlap between mini-isolated leptons and jets.

Scale factors that account for selection efficiency differences between data and simulation are calculated as a function of lepton p_T and η using a “tag-and-probe” method [31, 32, 59]. These were calculated in separate measurements for the single-lepton trigger, lepton identification, and I_{mini} requirements.

These scale factors are applied to simulated events for both lepton flavors. For the 2D isolation requirement, no significant difference is found between the selection efficiencies in data and simulation and hence no scale factor is applied.

4.2 Hadronic W and H tagging

In the decay of a heavy T quark, particles are produced with high momentum and large Lorentz boost. The decay products of top quarks and W, Z, or Higgs bosons are therefore often collimated. This can be seen in Fig. 2 in which the angular separation ΔR between the products of simulated $W \rightarrow q\bar{q}'$ and $H \rightarrow b\bar{b}$ decays are shown for several T quark masses. Even for the lightest considered mass point this separation often has values of $\Delta R < 0.8$, where the decay products of heavy bosons can merge into a single AK8 jet.

A jet shape variable called “N-subjettiness” [60], denoted as τ_N , is defined as the sum of the transverse momenta of k constituent particles weighted by their minimum angular separation from one of N subjet candidates ($\Delta R_{N,k}$), which are in a jet of characteristic radius R_0 :

$$\tau_N = \frac{1}{R_0 \sum_k p_{T,k}} \sum_k p_{T,k} \min(\Delta R_{1,k}, \Delta R_{2,k}, \dots, \Delta R_{N,k}). \quad (2)$$

This variable quantifies the consistency of a jet with originating from an N -prong particle decay. The ratio τ_2/τ_1 provides high sensitivity to two-prong decays such as $W \rightarrow qq'$. Jet grooming techniques (“pruning” and “soft drop”) are used to remove soft and wide-angle radiation so that the mass of the hard constituents can be measured more precisely [61, 62]. The pruning procedure reclusters the jet, removing soft or large-angle particles, while the soft drop algorithm recursively declusters the jet, removing sub-clusters until two subjets are identified within the AK8 jet. AK8 jets are reconstructed independently of AK4 jets, so they will

frequently overlap. Unless otherwise stated, such overlapping jets are not removed when applying selections based on jet multiplicity.

The AK4 jets and subjets of AK8 jets can be tagged as originating from b quarks based on information about secondary vertices and displaced tracks within the jet. The efficiency for tagging b hadron jets in simulation is approximately 65%, averaged over jet p_T (slightly lower for subjets of AK8 jets), and the probability of mistagging a charm (light) quark jet is 13% (1%) [63]. Scale factors, which are functions of jet p_T and flavor, are applied to account for efficiency differences between data and simulation.

An AK8 jet is labeled as “W tagged” if it has $p_T > 200$ GeV, $|\eta| < 2.4$, pruned jet mass between 65 and 105 GeV, and the ratio $\tau_2/\tau_1 < 0.6$. Differences in the pruned jet mass distribution and τ_2/τ_1 selection efficiency between data and simulation have been evaluated in Ref. [64]. To account for these differences, pruned jet mass scale factors and mass resolution smearing factors are applied in simulation to all AK8 jets. A τ_2/τ_1 selection scale factor is applied in simulation to jets that are spatially matched to true boosted products of a hadronic W boson decay.

Higgs boson candidate jets are reconstructed by exploiting the significant branching fraction of the Higgs boson to $b\bar{b}$ pairs. AK8 jets are marked as “H tagged” if they have $p_T > 300$ GeV, soft drop jet mass in the range 60–160 GeV, and if at least one of the two subjets from the soft drop algorithm is tagged as a bottom subjet.

5 Boosted H channel

5.1 Event selection and categorization

In this channel, one electron with $p_T > 50$ GeV and $|\eta| < 2.4$, or one muon with $p_T > 47$ GeV and $|\eta| < 2.1$ is required. In events with an electron, at least one AK4 jet with $p_T > 250$ GeV and a second AK4 jet with $p_T > 70$ GeV are required to select events with a nearly constant trigger efficiency. Furthermore, selected events must have $S_T > 800$ GeV, at least three AK4 jets, and at least two AK8 jets, since we expect a hadronic decay of a boosted Higgs boson in each event along with at least one other hadronic t quark, W, Z, or further Higgs boson decay. For the rejection of non top quark backgrounds, at least one b-tagged AK4 jet is required.

Distributions of the variables used in the H-tagging algorithm, as described in Section 4, are shown in Fig. 3. These distributions are from events that pass all selection criteria outlined above except for the b-tagging requirement, and that have the corrections described in Section 5.2 applied. The distribution of the number of b-tagged subjets for the highest p_T AK8 jet with soft drop jet mass within 60–160 GeV is shown along with the mass of the highest p_T AK8 jet with two b-tagged subjets, before the mass requirement. To illustrate the sensitivity of the H-tagging algorithm to the presence of boosted Higgs bosons, the $T\bar{T}$ signal with a mass of 1200 GeV is split into two curves: the solid curve shows $T\bar{T}$ events where at least one Higgs boson is present in the decay chain and the dashed curve shows $T\bar{T}$ events with only $T \rightarrow tZ$ or $T \rightarrow bW$ decays. It can be seen that signal events with at least one $T \rightarrow tH$ decay produce a clear peak at 125 GeV in the mass distribution of the H-tagged jet. Signal events without a Higgs boson in the decay chain have a less pronounced increase at 90 GeV because of hadronic Z boson decays.

After passing the selection defined above, events are split into two exclusive categories, which depend on the number of b-tagged subjets of H-tagged jets, and are defined as follows:

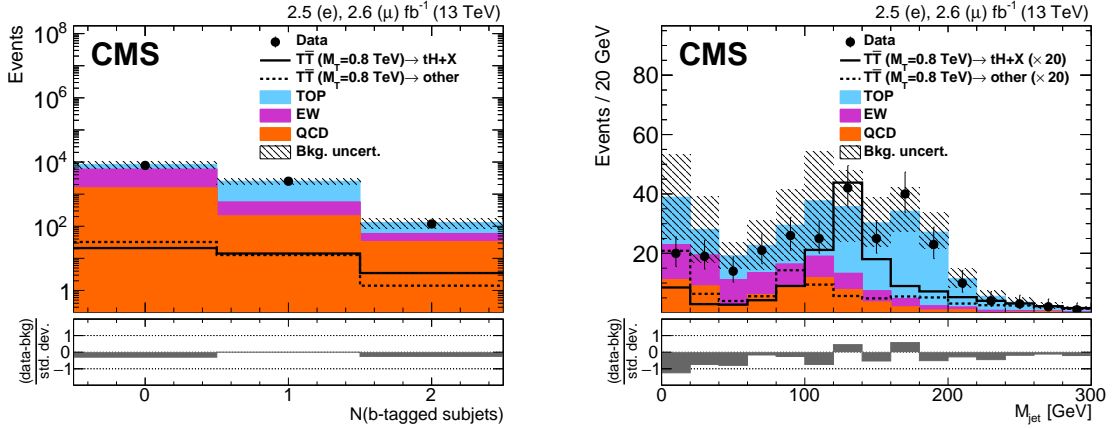


Figure 3: Distributions of the number of b-tagged subjects of the highest p_T H-tagged jet candidate with $p_T > 300$ GeV and M_{jet} in the range $[60, 160]$ GeV (left), and M_{jet} of the highest p_T H-tagged jet candidate with $p_T > 300$ GeV and two subject b tags (right). A T quark signal with $M(T) = 0.8$ TeV is shown (right), normalized to the predicted cross section and scaled by a factor of 20, with the singlet benchmark branching fractions assumed. The solid (dashed) curve shows $T\bar{T}$ events with at least one (zero) Higgs boson decay, where contributions from each decay mode are weighted to reflect the singlet branching fraction scenario. The uncertainty in the background includes the statistical and systematic uncertainties described in Section 7.

- H2b: events with at least one H-tagged jet with exactly *two* b-tagged subjects.
- H1b: events with at least one H-tagged jet with exactly *one* b-tagged subject.

To avoid an overlap between the two categories, any event is first checked whether it falls into the H2b category and only if it does not, it can enter into the H1b category.

5.2 Background modeling

To evaluate the modeling of $t\bar{t}$ and $W + \text{jets}$ production, the dominant background processes, two control regions that are enriched in events from these processes are defined by modifying the event selection defined in Section 5.1. In the $t\bar{t}$ control region, at least two b-tagged jets are required instead of at least one. In the $W + \text{jets}$ control region, the requirement of at least one b-tagged jet is inverted and events with any b-tagged jets are rejected. Events with an H-tagged jet are rejected in both control regions to reduce the signal contribution in these regions, and $E_T^{\text{miss}} > 100$ GeV is required to reject events from multijet production. The signal to background ratio is about six times smaller than the one in the H2b category in the $t\bar{t}$ control region and about 30 times smaller in the $W + \text{jets}$ control region. Events are corrected for all known sources of discrepancies between the data and simulation such as differing reconstruction or tagging efficiencies. It is observed that jets have a harder p_T spectrum in simulation, leading to significant discrepancies from observed distributions of quantities such as H_T . The discrepancies in both control regions are well described by 2-parameter linear fits with negative slopes to the ratio between data and simulation in the H_T distributions [65, 66]. Modeling of the $t\bar{t}$ and $W + \text{jets}$ background samples is corrected using the results of these fits. The S_T distributions for both control regions are shown in Fig. 4 with all corrections applied.

To evaluate the uncertainty in the normalization of the $t\bar{t}$ and $W + \text{jets}$ background processes, a binned maximum likelihood fit [67] of the background-only hypothesis is performed in the two control regions using the THETA framework [68]. All systematic uncertainties (discussed in more detail in Section 7) are accounted for, except for uncertainties in the rate of $t\bar{t}$ and

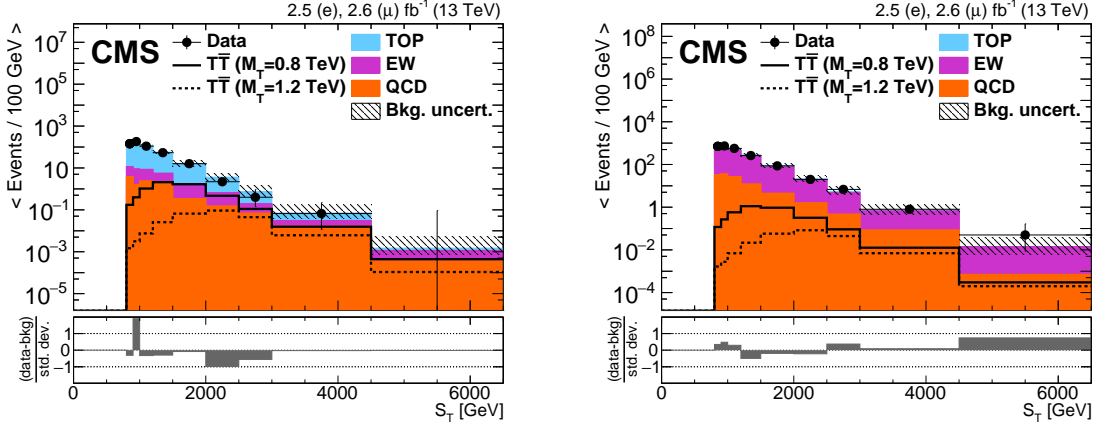


Figure 4: Distributions of S_T in the $t\bar{t}$ (left) and W + jets (right) control regions of the boosted H channel after applying all corrections to their shape and normalization. The $T\bar{T}$ signal, shown for T quark masses of 0.8 and 1.2 TeV, is normalized to the theoretical cross section and the singlet benchmark branching fractions are assumed. The uncertainty in the background includes statistical and systematic uncertainties described in Section 7.

W + jets backgrounds that are constrained using this fit. The resulting uncertainties in the normalizations of the two backgrounds are 8.7% for $t\bar{t}$ and 6% for W + jets. These uncertainties are included in the final statistical interpretation of the results (discussed in Section 8) as rate uncertainties. In both control regions, data and simulation agree within the systematic uncertainties described in Section 7.

6 Boosted W channel

6.1 Event selection

The selection in this channel is optimized for the identification of boosted W boson decays. Selected events are required to have no H -tagged jets ensuring that the event sample in this channel is complementary to that for the boosted Higgs channel, allowing a straightforward combination of the two channels. Events are selected that have one electron or muon, usually from the decay of a W boson in the $T \rightarrow bW$ decay mode or from a leptonic top quark decay in the $T \rightarrow tZ$ or tH decay modes. Electrons (muons) must have $p_T > 40$ GeV, $|\eta| < 2.1$ (2.4) and pass the tight identification and isolation requirements described in Section 4. Events having additional loose electrons or muons with $p_T > 10$ GeV are rejected.

Each event must have three or more AK4 jets, and the three highest p_T jets must satisfy $p_T > 300, 150,$ and 100 GeV, respectively. Since a neutrino is expected from a leptonic W boson decay, E_T^{miss} is required to be greater than 75 GeV, which also significantly reduces the background from multijet events. Control regions are separated from the signal region based on the angular separation between the lepton and the second-highest p_T jet in the event, $\Delta R(\ell, j_2)$. In both $T\bar{T}$ and background processes, the lepton is usually observed back-to-back with the highest transverse momentum AK4 jet, and in $T\bar{T}$ events the second-highest p_T jet also tends to be back-to-back with the lepton, as seen in Fig. 5. The signal region selection requires $\Delta R(\ell, j_2) > 1$. Figure 5 shows the distribution of $\Delta R(\ell, j_2)$ after all selection requirements except for $\Delta R(\ell, j_2) > 1$. All selection efficiency corrections for differences between data and simulation are applied, as well as the H_T -based reweighting described in Section 5.2.

To maximize sensitivity to the presence of $T\bar{T}$ production, events are divided into 16 categories

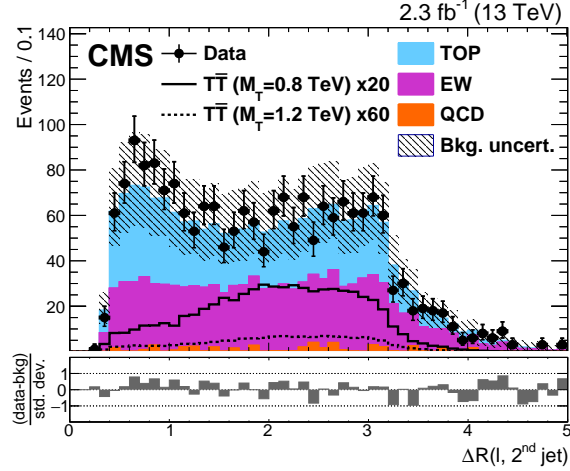


Figure 5: Distribution of $\Delta R(\ell, j_2)$ in the boosted W channel after all selection requirements except for $\Delta R(\ell, j_2) > 1$. Also shown are the distributions of $T\bar{T}$ signal events with T quark masses of 0.8 and 1.2 TeV, scaled by factors of 20 and 60, respectively. The uncertainty in the background includes the statistical and systematic uncertainties described in Section 7.

based on lepton flavor (e, μ), the number of b-tagged jets ($0, 1, 2, \geq 3$), and the number of boosted W-tagged jets ($0, \geq 1$). In events with no W-tagged jet, we require a fourth jet with $p_T > 30$ GeV. Figure 6 shows the distributions used for tagging boosted W bosons as well as the number of b-tagged and W-tagged jets. The pruned mass distribution for AK8 jets with $\tau_2/\tau_1 < 0.6$ shows a significant contribution of boosted W bosons in signal events weighted to correspond to the singlet branching fraction benchmark. The τ_2/τ_1 distribution in AK8 jets with pruned mass between 65–105 GeV shows that W + jets and multijet backgrounds are concentrated at higher values, as expected for jets without substructure.

We finally analyze the minimum mass constructed from the lepton (ℓ) and a b-tagged AK4 jet, labeled $\min[M(\ell, b)]$. In leptonic top quark decays, forming a mass from two of the three decay products, the lepton and b quark jet, produces a sharp edge near the top quark mass. Therefore this distribution is particularly suited to identifying $T \rightarrow bW$ decays, where the corresponding edge forms at much higher masses, near $M(T)$. In the categories with zero b-tagged AK4 jets, we consider the minimum mass of the lepton and any AK4 jet, denoted $\min[M(\ell, j)]$. This combination of discriminating variables provides the best sensitivity to low mass T quark production ($\lesssim 1$ TeV) in the singlet branching fraction scenario. Figure 7 shows distributions of $\min[M(\ell, j)]$ and $\min[M(\ell, b)]$ after the final selection but before the likelihood fits described in Section 8.

6.2 Background modeling

To cross check the modeling of background processes, we consider two control regions enriched by two dominant background processes, W + jets and $t\bar{t}$. To define these regions we invert the signal region requirement of $\Delta R(\ell, j_2) > 1$ and modify the requirement on the number of b-tagged jets to maximize either W + jets or $t\bar{t}$ yield. For an 800 GeV T quark we expect only 3 events in both control regions compared to a total background of 444, for a signal to background ratio that is a factor of ≈ 3 smaller than in the signal region.

The W + jets control region has zero b-tagged jets and events are categorized according to the number of W-tagged jets ($0, \geq 1$). The $t\bar{t}$ region has one or more b-tagged jets and events are categorized according to the number of b-tagged jets ($1, \geq 2$). Figure 8 shows distributions of $\min[M(\ell, j)]$ in the W + jets control region and $\min[M(\ell, b)]$ in the $t\bar{t}$ control region. Both re-

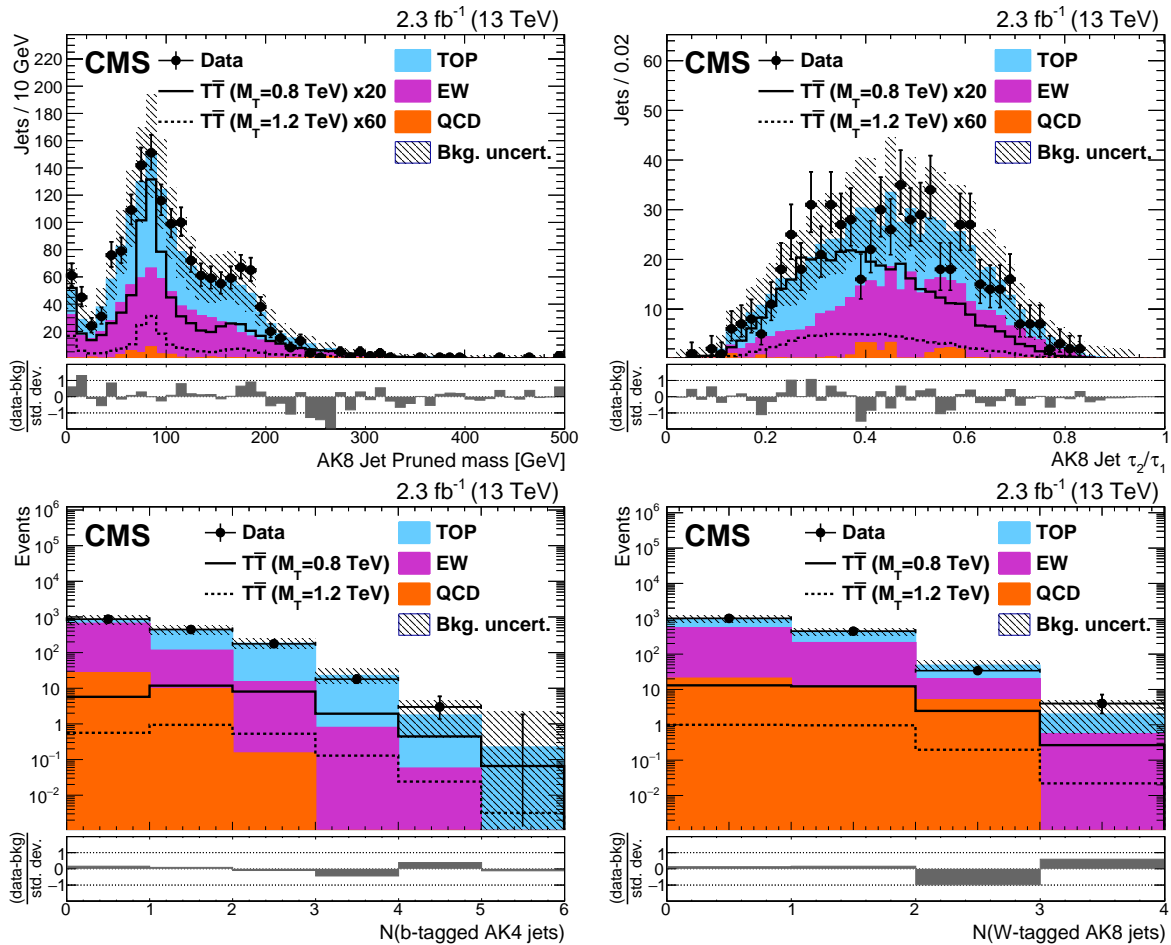


Figure 6: Distributions of (left-to-right, upper-to-lower) pruned jet mass for AK8 jets with $\tau_2/\tau_1 < 0.6$, τ_2/τ_1 for AK8 jets with pruned mass within 65–105 GeV, number of b-tagged AK4 jets, and number of W-tagged AK8 jets in the boosted W channel with all categories combined. Also shown are the distributions of $T\bar{T}$ signal events with T quark masses of 0.8 and 1.2 TeV, scaled by factors of 20 and 60, respectively, in the upper figures. The uncertainty in the background includes the statistical and systematic uncertainties described in Section 7.

gions show that simulation-based background predictions agree with data within the systematic uncertainties described in Section 7. Observed and predicted event yields in the control regions for all categories are compared as a closure test, and differences in yields are assigned as an additional systematic uncertainty. This uncertainty accounts for any background mis-modeling after selection and scale factor application.

7 Systematic uncertainties

We consider sources of systematic uncertainty that can affect the normalization and/or the shape of both background and signal distributions. A summary of these systematic uncertainties along with their numerical values and whether they are applied to signal or background samples can be found in Table 2.

The uncertainty in the integrated luminosity is 2.3% [69] and is applied to all simulated samples. Normalization uncertainties in the rates of SM processes include 20% for single top quark production and 15% for diboson production, based on CMS measurements [70, 71]. For multijet

production a rate uncertainty of 100% is assigned in the boosted H channel since the simulation used in this channel does not contain either the PDF or matrix element scale uncertainties, unlike those used in the boosted W channel. No rate uncertainty is applied to Z + jets production since for this process experimental and theoretical uncertainties are small compared to the energy scale and PDF uncertainties described below. Additionally, both channels derive normalization uncertainties for $t\bar{t}$ and W + jets samples from control regions, with values of 5–12% and 4–20% in the boosted W channel, and 8.7% and 6.0% in the boosted H channel. Trigger, lepton identification, and lepton isolation efficiency scale factor uncertainties are also applied as normalization uncertainties.

Uncertainties in both channels affecting the shape and normalization of the distributions include uncertainties related to jet energy scale, jet energy resolution, pruned or soft drop jet mass scale and resolution, and b tagging and light-flavor mistagging efficiencies. These are evaluated by raising and lowering their values with respect to the central values by one standard deviation of the respective uncertainties and recreating a distribution using shifted values at each step of the analysis. An additional uncertainty of 5% is applied in the boosted H channel to account for potential differences when propagating the jet mass scale and resolution scale factors, measured using hadronic W boson decays, to Higgs boson candidate jets. This uncertainty has been determined by comparing samples simulated with the PYTHIA 8 and HERWIG++ [72] (with the CUETP8M1 tune [53, 54]) hadronization programs and evaluating the difference between the two programs in the jet mass distributions for hadronically decaying W and Higgs bosons. In the boosted W channel we also apply shape uncertainties to the W boson tagging corrections for the τ_2/τ_1 selection efficiency and its p_T dependence. To account for small differences in the H-tagging efficiency between the boosted W and boosted H channel, a 3% normalization uncertainty is assigned that is correlated with the b tagging uncertainty in the boosted H channel and anticorrelated in the boosted W channel.

The uncertainty due to pileup modeling is evaluated by varying by $\pm 5\%$ the total inelastic cross section used to calculate the pileup distribution. The systematic uncertainty in the H_T -based background reweighting procedure is taken to be the difference between the unweighted distribution and a distribution where the correction factor is applied twice.

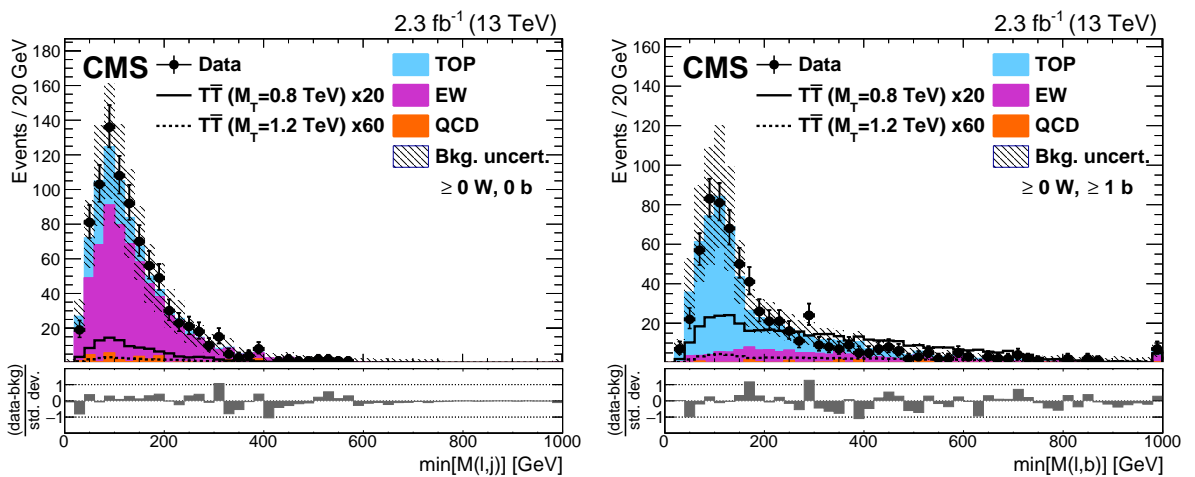


Figure 7: Distributions of $\min[M(\ell, j)]$ in events without b-tagged AK4 jets (left) and $\min[M(\ell, b)]$ in events with ≥ 1 b-tagged AK4 jets (right) in the boosted W channel with all categories combined. Also shown are the distributions of $T\bar{T}$ signal events with T quark masses of 0.8 and 1.2 TeV, scaled by factors of 20 and 60, respectively. The uncertainty in the background includes the statistical and systematic uncertainties described in Section 7.

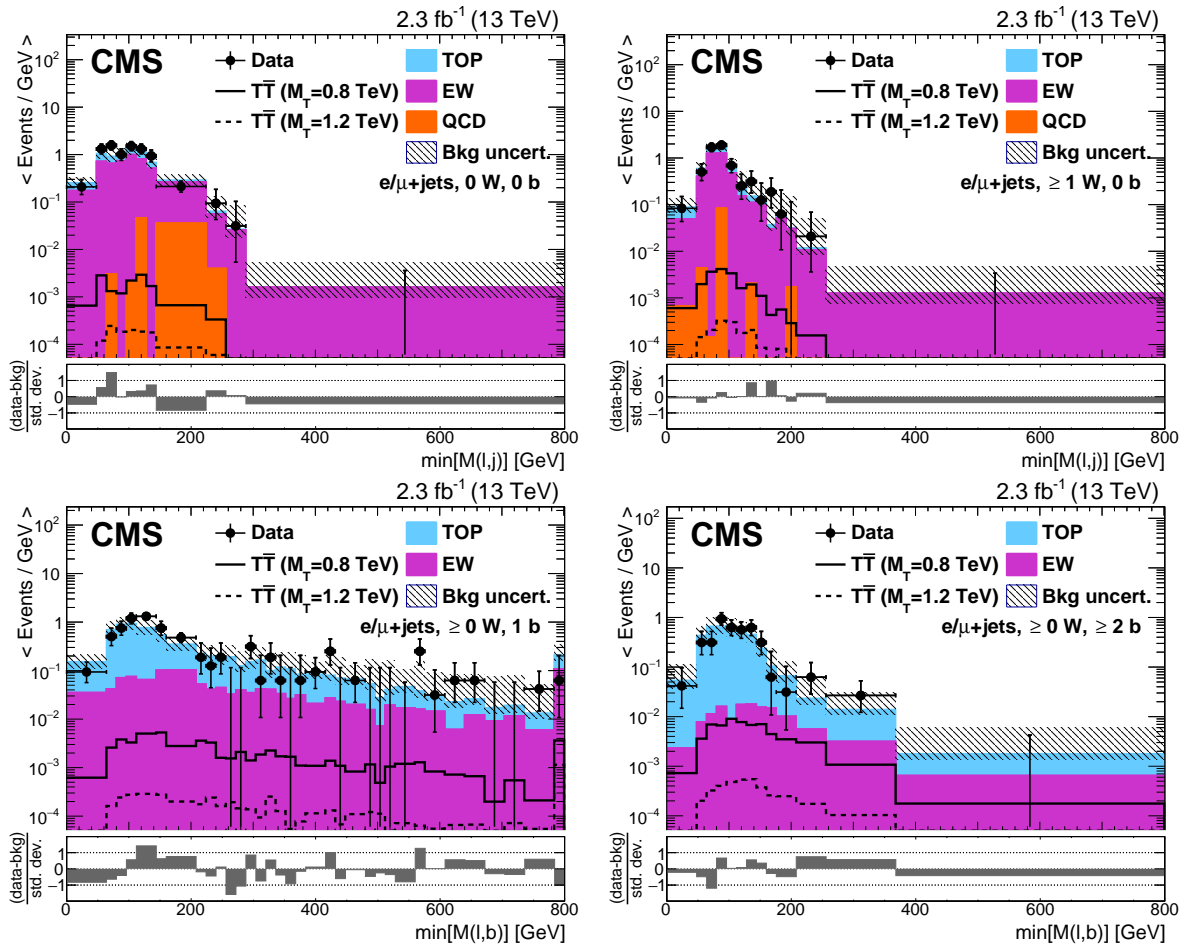


Figure 8: Distributions of $\min[M(\ell, j)]$ in the $W + \text{jets}$ control region of the boosted W channel (upper) for $0/\geq 1$ W tag categories (left/right), and $\min[M(\ell, b)]$ in the $t\bar{t}$ control region of the boosted W channel (lower) for $1/\geq 2$ b tag categories (left/right). Also shown are the distributions of $t\bar{t}$ signal events with T quark masses of 0.8 and 1.2 TeV. The uncertainty in the background includes the statistical and systematic uncertainties described in Section 7.

The uncertainties in the PDFs used in MC simulation are evaluated from the set of NNPDF3.0 fitted replicas, following the standard procedure [55]. Renormalization and factorization scale uncertainties are calculated by varying the corresponding scales up or down (either independently or simultaneously) by a factor of two and taking as uncertainty the envelope, or largest spread, of all possible variations. These theoretical uncertainties are applied to the signal simulation as shape uncertainties, together with small normalization uncertainty contributions due to changes in acceptance.

The PDF and scale variation uncertainties affect both the normalization and shape of background distributions for multijet (in the boosted W channel), $Z + \text{jets}$, and single top quark MC samples. For the $t\bar{t}$ and $W + \text{jets}$ backgrounds the theoretical and H_T reweighting uncertainties dominate the total uncertainty in this search, and theoretical uncertainties are treated differently across the two channels. Changes of energy scale or parton momentum strongly influence H_T and therefore these uncertainties are correlated with the uncertainty in the H_T reweighting method. In the boosted H channel, only the uncertainty in the H_T reweighting procedure is considered as this uncertainty dominates over energy scale variations and PDF uncertainties, especially in the tails of the S_T distribution. In the boosted W channel the uncertainty in the H_T

Table 2: Summary of the systematic uncertainties, along with numerical values and application to signal and/or background samples. The second column gives the magnitude of normalization uncertainties or the procedure used to evaluate shape uncertainties. The symbol σ indicates one standard deviation of the corresponding systematic uncertainty. Renormalization and factorization energy scale uncertainties are treated as shape-only for signal but include normalization uncertainties in background. Values stated for shape uncertainties indicate a representative range over the categories for the dominant backgrounds and/or signal.

Source	Uncertainty		Signal	Background	
	Boosted W	Boosted H		Boosted W	Boosted H
Int. luminosity		2.3%	Yes	All	All
Diboson rate		15%	No	diboson	diboson
Single t quark rate		20%	No	t	t
QCD rate	—	100%	No	—	QCD
$t\bar{t}$ rate	5–12%	8.7%	No	$t\bar{t}$	$t\bar{t}$
W + jets rate	4–20%	6.0%	No	W + jets	W + jets
Trigger (e)	5%	2%	Yes	All	All
Trigger (μ)	5%	1%	Yes	All	All
Identification (e, μ)	1%	2%	Yes	All	All
Isolation (e, μ)	1%	—	Yes	All	—
Pileup	$\sigma_{\text{inel.}} \pm 5\%$		Yes	All (0–3%)	All (0–3%)
Jet energy scale	$\pm\sigma(p_T, \eta)$		Yes	All (0–12%)	All (0–4%)
Jet energy res.	$\pm\sigma(\eta)$		Yes	All (0–8%)	All (0–1%)
H_T reweighting	envelope(no weight, weight squared)		No	$t\bar{t}$, W + jets, QCD (17–34%)	$t\bar{t}$, W + jets (13–21%)
b tag: b	$\pm\sigma(p_T)$		Yes	All (0–16%)	All (3–8%)
b tag: light flavors	$\pm\sigma$		Yes	All (0–6%)	All (1–4%)
W/H tag: mass scale	$\pm\sigma(p_T, \eta)$		Yes	All (0–3%)	All (0–7%)
W/H tag: mass res.	$\pm\sigma(\eta)$		Yes	All (0–5%)	All (0–7%)
H tag: efficiency	3%		Yes	All	All
H tag: propagation	—	5%	Yes	—	All
W tag: τ_2/τ_1	$\pm\sigma$		Yes	All (0–2%)	—
W tag: $\tau_2/\tau_1 p_T$	$\pm\sigma(p_T)$		Yes	All (0–2%)	—
Renorm./fact. scale	envelope ($\times 2, \times 0.5$)		Shape	All (22–44%)	Z + jets, t (2–23%)
PDF	$\pm\sigma$		Shape	Z + jets, t, QCD (1–7%)	Z + jets, t (0–13%)

reweighting dominates over the PDF uncertainty, but is comparable in shape and magnitude to the scale variation uncertainty, with scale variations providing the dominant uncertainty at low values of $\min[M(\ell, b)]$. In this channel both H_T reweighting and scale variation uncertainties are considered for $t\bar{t}$ and W + jets backgrounds. All of these shared uncertainties are treated as correlated between the two analysis channels in the statistical interpretation of the results.

8 Results

Signal efficiencies for all possible final states of $T\bar{T}$ and $B\bar{B}$ production in the boosted W and boosted H channels (after combining all categories in each channel) are listed in Table 3 for two signal hypotheses with a high and a low vector-like quark mass. The values are derived by dividing the number of signal events that have the corresponding decay mode in each category by the number of expected events in the same decay mode before any selection. It can be seen that the selection applied in the boosted H channel is most efficient if a Higgs boson is present in the final state, whereas the selection in the boosted W channel favors $T \rightarrow bW$ decays, thus showing how the combination of the two channels improves sensitivity to most branching

Table 3: Signal efficiencies in the boosted W and boosted H event categories, split into the six possible final states, of both $T\bar{T}$ and $B\bar{B}$ production for two illustrative mass points. Efficiencies are calculated with respect to the expected number of events in the corresponding final state before any selection. The relative uncertainty in the efficiencies after combining systematic and statistical uncertainties in the MC samples is about 8% in the boosted W categories and about 12% in the boosted H categories.

Production process	Decay mode	Boosted W categories	Boosted H categories
$T\bar{T}$ (0.8 TeV)	tHtH	2.9%	8.7%
	tHtZ	3.2%	7.3%
	tHbW	5.8%	6.3%
	tZtZ	3.7%	5.6%
	tZbW	6.3%	4.2%
	bWbW	10.0%	2.5%
$T\bar{T}$ (1.2 TeV)	tHtH	3.6%	10.5%
	tHtZ	4.1%	9.0%
	tHbW	7.3%	7.1%
	tZtZ	4.7%	6.7%
	tZbW	8.3%	4.8%
	bWbW	13.2%	2.5%
$B\bar{B}$ (0.8 TeV)	bHbH	1.7%	1.9%
	bHbZ	1.3%	1.9%
	bHtW	5.8%	6.1%
	bZbZ	0.8%	1.4%
	bZtW	6.4%	4.2%
	tWtW	7.9%	5.7%
$B\bar{B}$ (1.2 TeV)	bHbH	1.7%	2.1%
	bHbZ	1.4%	1.9%
	bHtW	7.3%	7.1%
	bZbZ	0.8%	1.5%
	bZtW	8.2%	4.7%
	tWtW	11.4%	7.0%

fraction combinations of the T quark. For B quark decays the boosted W channel has high efficiency for the tW decays and reduced efficiency for the bZ/bH decays owing to the lack of semileptonic top quark decays. Similarly, the boosted H channel is most efficient for the bHtW final state since a leptonic decay is required as well as an H-tag.

In Fig. 9, $\min[M(\ell, j)]$ or $\min[M(\ell, b)]$ distributions are shown for each of the 8 tagging categories in the boosted W channel after the final event selection, with the electron and muon channels combined. Figure 10 shows distributions of S_T in the H1b and H2b categories after combining the electron and muon channels. As these two variables provide good discrimination between signal and background in their respective categories, they are used for the final statistical interpretation of the data. In all plots, the $T\bar{T}$ signal distributions assume the singlet benchmark branching fractions. The event yields are given in Table 4.

After the final event selection, no significant excess above the SM expectations is observed in data. We set 95% CL upper limits on the cross section of $T\bar{T}$ production in various branching fraction scenarios. These limits are defined as Bayesian credible intervals [67] and are derived using the THETA [68] program. Statistical uncertainties due to the finite size of the MC samples are accounted for using the Barlow–Beeston lite method [73]. Systematic uncertainties are

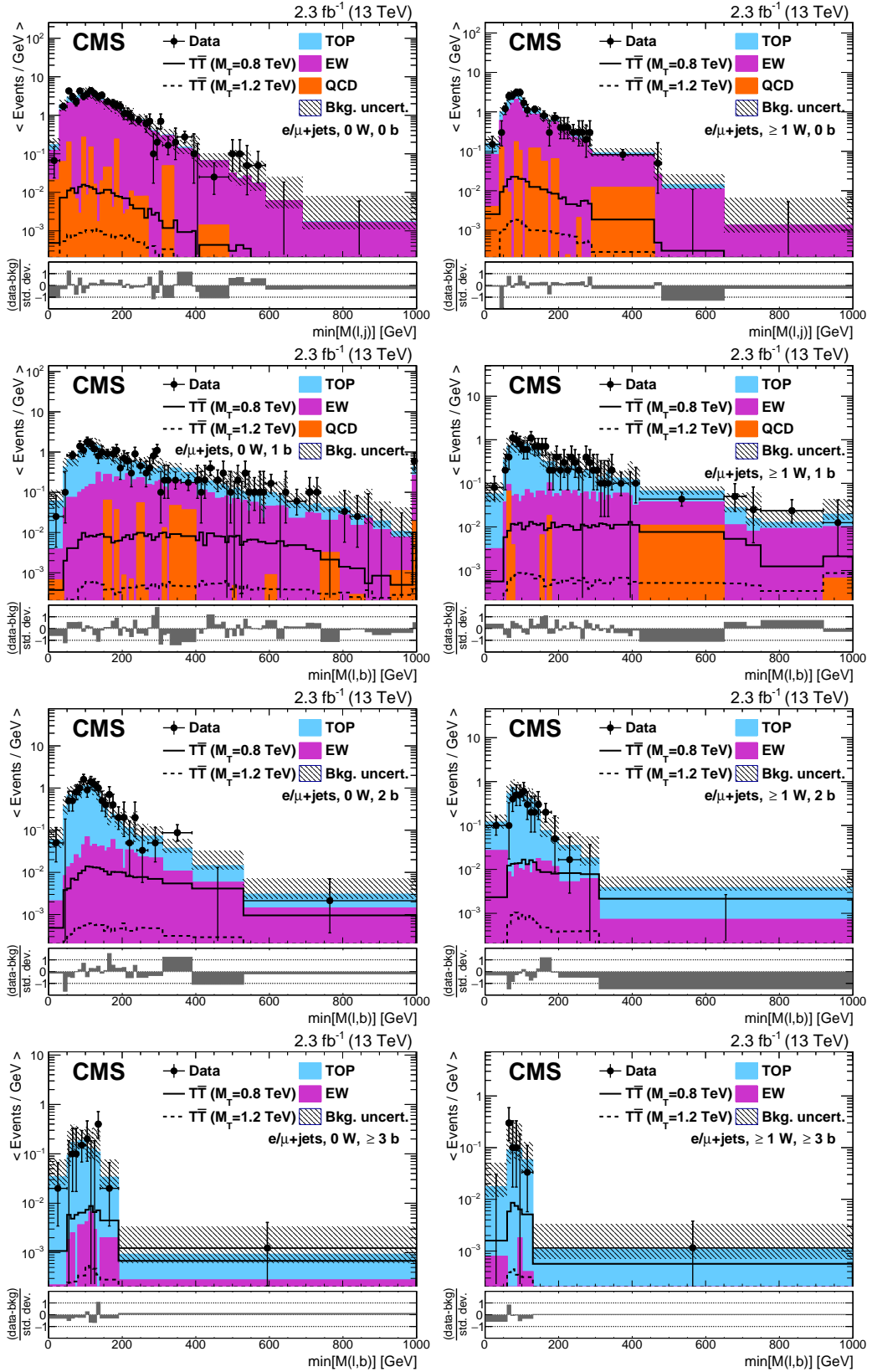


Figure 9: Distributions of $\min[M(\ell, j)]$ or $\min[M(\ell, b)]$ in the combination of electron and muon channels in the boosted W categories with 0 (left) or ≥ 1 (right) W-tagged jets and (upper to lower) 0, 1, 2, or ≥ 3 b-tagged jets. Also shown are the distributions of $T\bar{T}$ signal events with T quark masses of 0.8 and 1.2 TeV. The uncertainty in the background includes the statistical and systematic uncertainties described in Section 7.

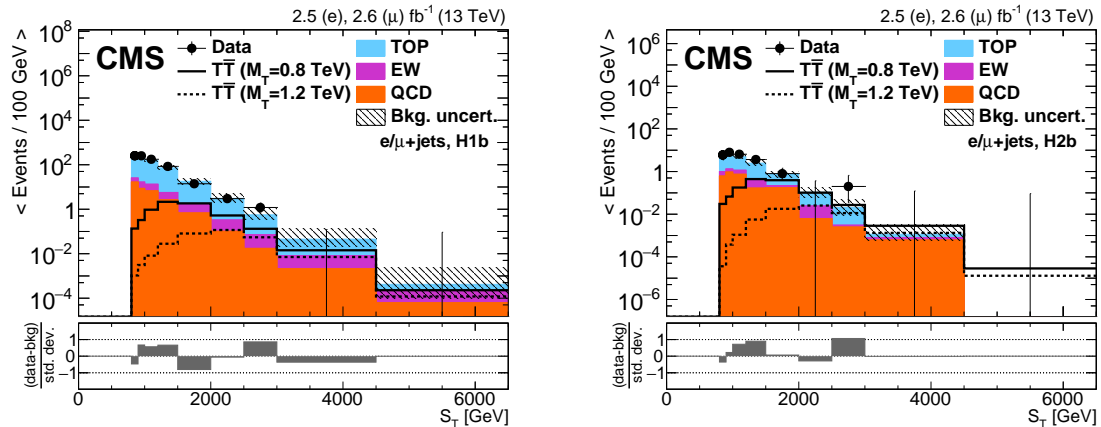


Figure 10: Distributions of S_T in the H1b (left) and H2b (right) categories in the combination of electron and muon channels. The $T\bar{T}$ signal, shown for T quark masses of 0.8 and 1.2 TeV, is normalized to the theoretical cross section and the singlet benchmark branching fractions are assumed. The uncertainty in the background includes the statistical and systematic uncertainties described in Section 7.

treated as nuisance parameters with log-normal priors for normalization uncertainties, Gaussian priors for shape uncertainties with shifted templates, and a flat prior on the signal cross section. The limits are then calculated by simultaneously fitting the binned marginal likelihoods obtained from the $\min[M(\ell, b)]$ distributions in all boosted W categories and the S_T distributions in all boosted H categories. This creates a combined search with 20 categories after dividing into electron and muon channels: 16 categories from the boosted W channel and 4 categories with a boosted Higgs boson. The systematic uncertainties for these categories are correlated, as described in Section 7.

Results for the individual channels are shown in Fig. 11. The boosted W channel excludes T quarks decaying only to bW with masses below 910 GeV (870 GeV expected), and the boosted H channel excludes T quarks decaying only to tH for masses below 890 GeV (860 GeV expected). In Fig. 12 we present combined 95% CL upper limits on the $T\bar{T}$ production cross section for two VLQ benchmark branching fraction combinations: singlet (50% bW , 25% tZ/tH) and doublet (50% tZ/tH). For an electroweak singlet T quark, the observed (expected) upper limits on the production cross section range from 0.26 to 0.04 pb (0.31 to 0.04 pb) and we exclude masses below 860 GeV (790 GeV). For a doublet T quark, the observed (expected) upper limits on the production cross section range from 0.37 to 0.04 pb (0.34 to 0.03 pb) and we exclude masses below 830 GeV (780 GeV). The corresponding benchmarks for B quark production are shown in Fig. 13, and we can exclude masses below 730 GeV (720 GeV expected) for the singlet branching fraction combination while for the doublet scenario, no lower mass limit above 700 GeV was observed. Sensitivity to $B\bar{B}$ production in this search is limited by the single lepton selection efficiency for bZ and bH decays, as noted above. The combinations benefit from the difference in discriminating variables between the channels: the $\min[M(\ell, b)]$ distributions used in the boosted W channel provide good sensitivity to low-mass T quarks, while the peaking signal shape in the S_T distribution drives the combination at high masses. The observed exclusion limits are stronger than expected due to an over-prediction of the background that remains after the H_T -based reweighting, particularly in categories with a W -tagged jet and several b -tagged jets. This effect is not significant given the systematic uncertainty in the reweighting procedure.

Table 4: Number of events in each category after combining the electron and muon channels. Uncertainties include statistical and systematic components from Table 2, with uncertainty in the total background yield accounting for correlations across background processes. Yields of $T\bar{T}$ signal assume the theoretically predicted production cross section within the singlet branching fraction scenario.

Sample	0 W, 0 b	0 W, 1 b	0 W, 2 b	0 W, ≥ 3 b
$T\bar{T}$ (0.8 TeV)	2.5 ± 0.7	5.3 ± 1.3	3.9 ± 1.0	1.4 ± 0.4
$T\bar{T}$ (1.2 TeV)	0.23 ± 0.06	0.42 ± 0.11	0.26 ± 0.07	0.09 ± 0.02
TOP	103 ± 41	205 ± 78	111 ± 41	16.3 ± 6.8
EW	460 ± 160	80 ± 30	10.7 ± 4.0	0.6 ± 0.2
QCD	14.1 ± 6.3	6.2 ± 3.7	<1	<1
Total bkg.	570 ± 170	292 ± 84	122 ± 41	16.9 ± 6.8
Data	588	288	131	14

Sample	≥ 1 W, 0 b	≥ 1 W, 1 b	≥ 1 W, 2 b	≥ 1 W, ≥ 3 b
$T\bar{T}$ (0.8 TeV)	3.3 ± 0.9	6.6 ± 1.7	4.2 ± 1.1	1.0 ± 0.3
$T\bar{T}$ (1.2 TeV)	0.34 ± 0.09	0.52 ± 0.13	0.27 ± 0.07	0.06 ± 0.02
TOP	71 ± 26	111 ± 42	56 ± 20	7.6 ± 3.3
EW	180 ± 50	29.0 ± 8.4	4.4 ± 2.0	0.2 ± 0.1
QCD	12.6 ± 7.0	3.5 ± 2.6	0.2 ± 0.2	<1
Total bkg.	263 ± 57	143 ± 43	60 ± 20	7.8 ± 3.3
Data	274	155	45	7

Sample	H1b category	H2b category
$T\bar{T}$ (0.8 TeV)	21.5 ± 2.1	4.4 ± 0.7
$T\bar{T}$ (1.2 TeV)	1.5 ± 0.2	0.31 ± 0.05
TOP	1050 ± 220	29.6 ± 8.6
EW	45 ± 11	2.5 ± 0.9
QCD	50 ± 55	4.4 ± 5.1
Total bkg.	1150 ± 260	37 ± 12
Data	1204	43

Figure 14 shows expected and observed exclusion limits at 95% CL on the T quark mass, for a scan of possible branching fractions: we set lower mass limits with values ranging from 790 to 940 GeV for combinations with $\mathcal{B}(T \rightarrow tH) + \mathcal{B}(T \rightarrow bW) \geq 0.4$. Compared to the combination of many leptonic and hadronic search channels in $\sqrt{s} = 8$ TeV collision data corresponding to an integrated luminosity of 19.7 fb^{-1} , the current combination of two single lepton channels produces similar expected exclusion limits. This represents an improved sensitivity to $T\bar{T}$ pair production at $\sqrt{s} = 13$ TeV due to the increase in the $T\bar{T}$ production cross section from 8 to 13 TeV as well as to significant improvements in techniques for identifying boosted hadronic massive-particle decays. For branching fraction scenarios with $\mathcal{B}(T \rightarrow tH) + \mathcal{B}(T \rightarrow bW) \geq 0.4$ these results extend the excluded mass range of the 8 TeV search by up to 160 GeV.

9 Summary

The first search by CMS for pair-produced vector-like T and B quarks at $\sqrt{s} = 13$ TeV is presented, using data from proton-proton collisions recorded in 2015 corresponding to integrated luminosities of $2.3\text{--}2.6 \text{ fb}^{-1}$. The search requires at least one lepton in the final state and is op-

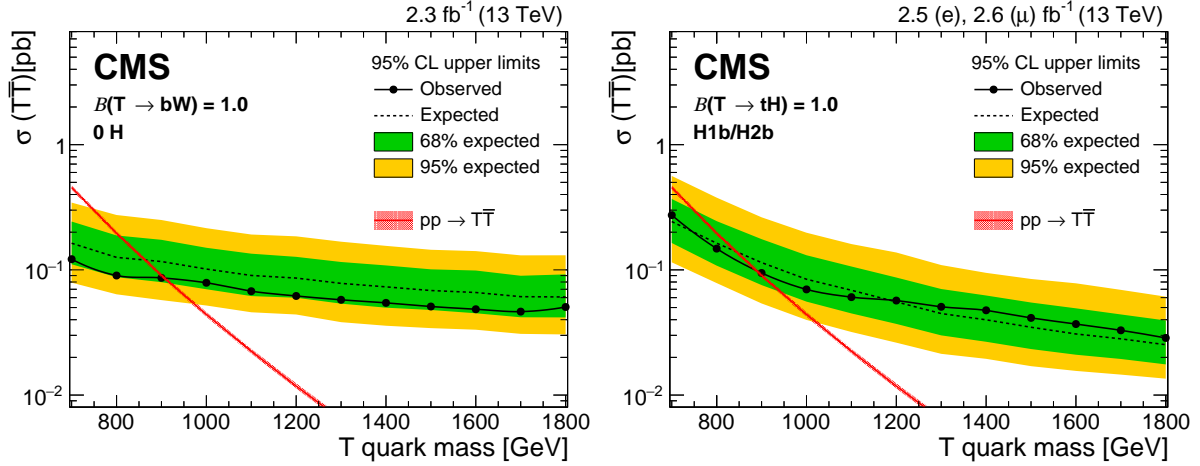


Figure 11: The expected and observed upper limits (Bayesian) at 95% CL on the cross section of $T\bar{T}$ production for 100% $T \rightarrow bW$ in the boosted W channel (left), and 100% $T \rightarrow tH$ in the boosted H channel (right). The theoretically predicted cross section for $T\bar{T}$ production calculated at NNLO is shown as red line, with the uncertainties in the PDFs and renormalization and factorization scales indicated by the shaded area. Masses below 700 GeV were excluded previously.

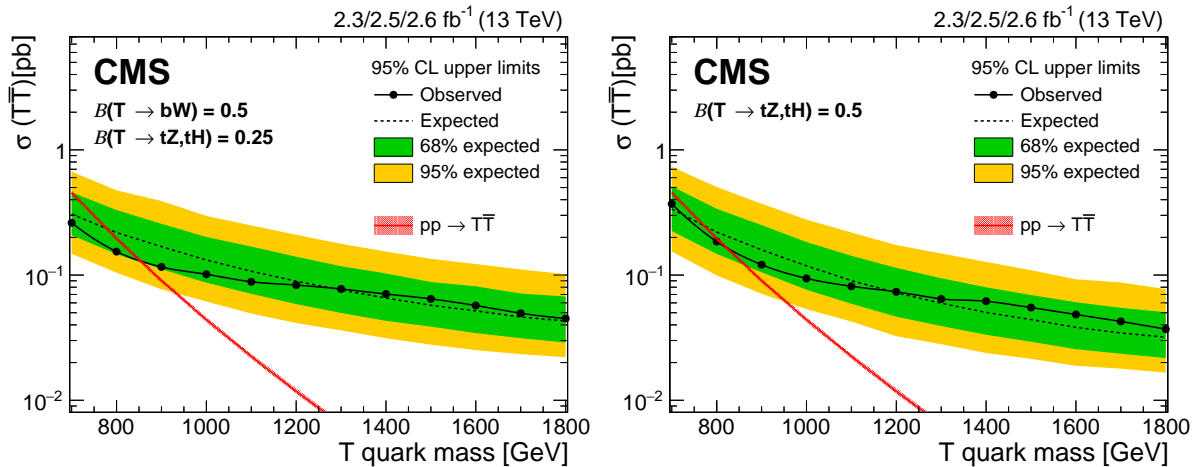


Figure 12: The expected and observed upper limits (Bayesian) at 95% CL on the cross section of $T\bar{T}$ production for the singlet benchmark (left) and the doublet benchmark (right) after combining the boosted W and boosted H channels. The theoretically predicted cross section for $T\bar{T}$ production calculated at NNLO is shown as red line, with the uncertainties in the PDFs and renormalization and factorization scales indicated by the shaded area. Masses below 700 GeV were excluded previously.

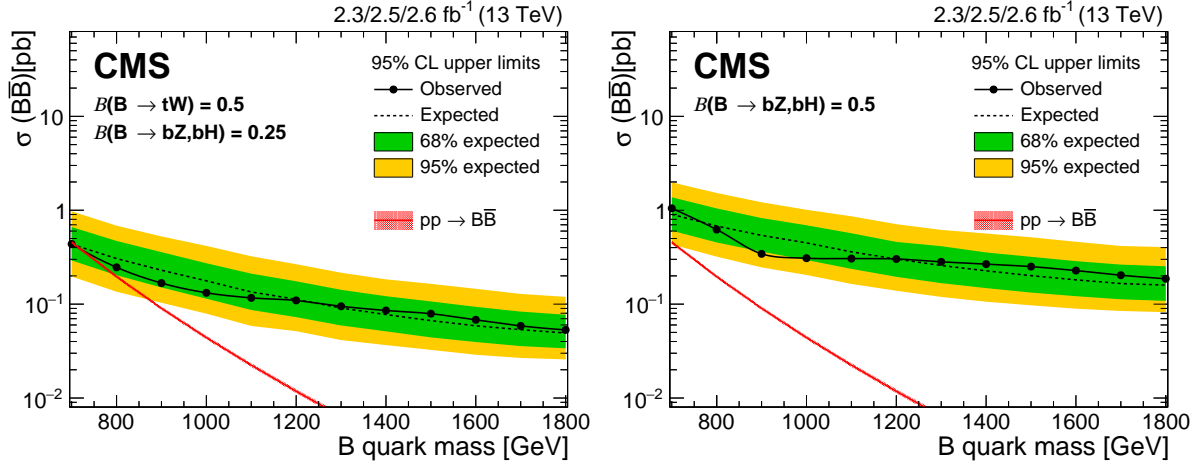


Figure 13: The expected and observed upper limits (Bayesian) at 95% CL on the cross section of $\text{B}\bar{\text{B}}$ production for the singlet benchmark (left) and the doublet benchmark (right) after combining the boosted W and boosted H channels. The theoretically predicted cross section for $\text{B}\bar{\text{B}}$ production calculated at NNLO is shown as red line, with the uncertainties in the PDFs and renormalization and factorization scales indicated by the shaded area. Masses below 700 GeV were excluded previously.

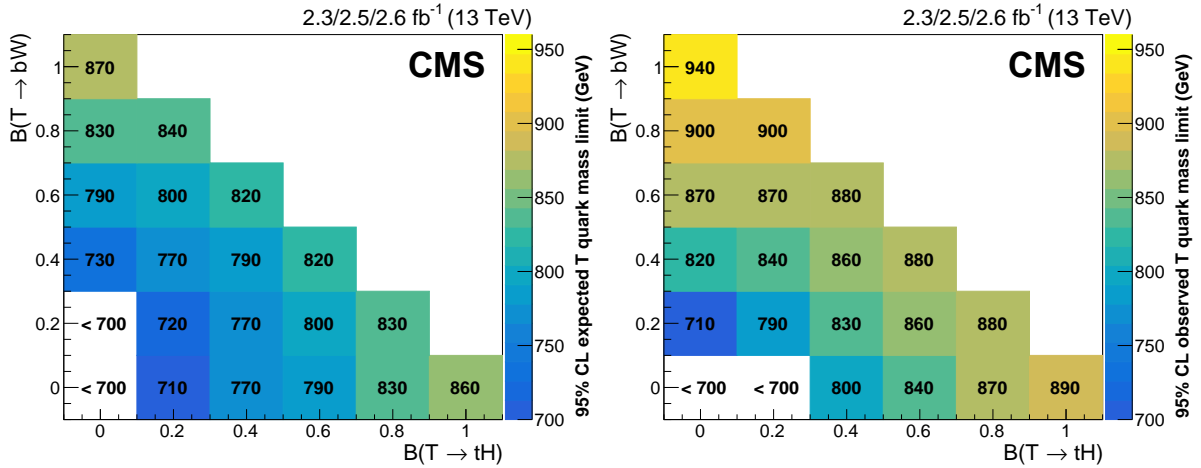


Figure 14: The expected (left) and observed (right) at 95% CL lower limits (Bayesian) on the T quark mass for a variety of $\text{T} \rightarrow \text{tH}$ and $\text{T} \rightarrow \text{bW}$ branching fraction combinations, indicated by the coordinates at the center of each box, after combining the boosted W and boosted H channels. A limit of <700 GeV indicates that this search is not sensitive to T quark decays with that branching fraction combination.

timized for cases where a T quark decays to a boosted W or Higgs boson. No excess above the standard model background is observed and 95% confidence level upper limits are placed on the cross section of $T\bar{T}$ and $B\bar{B}$ production. For an electroweak singlet T quark, masses below 860 GeV are excluded, and for a doublet T quark, masses below 830 GeV are excluded. Considering other possible branching fraction combinations for T quarks, and assuming that the sum of the branching fractions to bW , tH and tZ is equal to unity, we set lower mass limits that range from 790 to 940 GeV for combinations with $\mathcal{B}(T \rightarrow tH) + \mathcal{B}(T \rightarrow bW) \geq 0.4$. These results extend the sensitivity of previous CMS searches for many possible T quark decay scenarios, and showcase the importance of new techniques for understanding highly-boosted final states in extending searches for new particles to higher masses.

Acknowledgments

We congratulate our colleagues in the CERN accelerator departments for the excellent performance of the LHC and thank the technical and administrative staffs at CERN and at other CMS institutes for their contributions to the success of the CMS effort. In addition, we gratefully acknowledge the computing centers and personnel of the Worldwide LHC Computing Grid for delivering so effectively the computing infrastructure essential to our analyses. Finally, we acknowledge the enduring support for the construction and operation of the LHC and the CMS detector provided by the following funding agencies: BMWFW and FWF (Austria); FNRS and FWO (Belgium); CNPq, CAPES, FAPERJ, and FAPESP (Brazil); MES (Bulgaria); CERN; CAS, MoST, and NSFC (China); COLCIENCIAS (Colombia); MSES and CSF (Croatia); RPF (Cyprus); SENESCYT (Ecuador); MoER, ERC IUT, and ERDF (Estonia); Academy of Finland, MEC, and HIP (Finland); CEA and CNRS/IN2P3 (France); BMBF, DFG, and HGF (Germany); GSRT (Greece); OTKA and NIH (Hungary); DAE and DST (India); IPM (Iran); SFI (Ireland); INFN (Italy); MSIP and NRF (Republic of Korea); LAS (Lithuania); MOE and UM (Malaysia); BUAP, CINVESTAV, CONACYT, LNS, SEP, and UASLP-FAI (Mexico); MBIE (New Zealand); PAEC (Pakistan); MSHE and NSC (Poland); FCT (Portugal); JINR (Dubna); MON, RosAtom, RAS, RFBR and RAEP (Russia); MESTD (Serbia); SEIDI, CPAN, PCTI and FEDER (Spain); Swiss Funding Agencies (Switzerland); MST (Taipei); ThEPCenter, IPST, STAR, and NSTDA (Thailand); TUBITAK and TAEK (Turkey); NASU and SFFR (Ukraine); STFC (United Kingdom); DOE and NSF (USA).

Individuals have received support from the Marie-Curie program and the European Research Council and Horizon 2020 Grant, contract No. 675440 (European Union); the Leventis Foundation; the A. P. Sloan Foundation; the Alexander von Humboldt Foundation; the Belgian Federal Science Policy Office; the Fonds pour la Formation à la Recherche dans l'Industrie et dans l'Agriculture (FRIA-Belgium); the Agentschap voor Innovatie door Wetenschap en Technologie (IWT-Belgium); the Ministry of Education, Youth and Sports (MEYS) of the Czech Republic; the Council of Science and Industrial Research, India; the HOMING PLUS program of the Foundation for Polish Science, cofinanced from European Union, Regional Development Fund, the Mobility Plus program of the Ministry of Science and Higher Education, the National Science Center (Poland), contracts Harmonia 2014/14/M/ST2/00428, Opus 2014/13/B/ST2/02543, 2014/15/B/ST2/03998, and 2015/19/B/ST2/02861, Sonata-bis 2012/07/E/ST2/01406; the National Priorities Research Program by Qatar National Research Fund; the Programa Clarín-COFUND del Principado de Asturias; the Thalís and Aristeia programs cofinanced by EU-ESF and the Greek NSRF; the Rachadapisek Sompot Fund for Postdoctoral Fellowship, Chulalongkorn University and the Chulalongkorn Academic into Its 2nd Century Project Advancement Project (Thailand); and the Welch Foundation, contract C-1845.

References

- [1] ATLAS Collaboration, "Observation of a new particle in the search for the Standard Model Higgs boson with the ATLAS detector at the LHC", *Phys. Lett. B* **716** (2012) 1, doi:10.1016/j.physletb.2012.08.020, arXiv:1207.7214.
- [2] CMS Collaboration, "Observation of a new boson at a mass of 125 GeV with the CMS experiment at the LHC", *Phys. Lett. B* **716** (2012) 30, doi:10.1016/j.physletb.2012.08.021, arXiv:1207.7235.
- [3] CMS Collaboration, "Observation of a new boson with mass near 125 GeV in pp collisions at $\sqrt{s} = 7$ and 8 TeV", *JHEP* **06** (2013) 081, doi:10.1007/JHEP06(2013)081, arXiv:1303.4571.
- [4] L. Evans and P. Bryant, "LHC Machine", *JINST* **3** (2008) S08001, doi:10.1088/1748-0221/3/08/S08001.
- [5] M. Perelstein, M. E. Peskin, and A. Pierce, "Top quarks and electroweak symmetry breaking in little Higgs models", *Phys. Rev. D* **69** (2004) 075002, doi:10.1103/PhysRevD.69.075002, arXiv:hep-ph/0310039.
- [6] O. Matsedonskyi, G. Panico, and A. Wulzer, "Light top partners for a light composite Higgs", *JHEP* **01** (2013) 164, doi:10.1007/JHEP01(2013)164, arXiv:1204.6333.
- [7] R. Contino, L. Da Rold, and A. Pomarol, "Light custodians in natural composite Higgs models", *Phys. Rev. D* **75** (2007) 055014, doi:10.1103/PhysRevD.75.055014, arXiv:hep-ph/0612048.
- [8] R. Contino, T. Kramer, M. Son, and R. Sundrum, "Warped/composite phenomenology simplified", *JHEP* **05** (2007) 074, doi:10.1088/1126-6708/2007/05/074, arXiv:hep-ph/0612180.
- [9] D. B. Kaplan, "Flavor at SSC energies: A new mechanism for dynamically generated fermion masses", *Nucl. Phys. B* **365** (1991) 259, doi:10.1016/S0550-3213(05)80021-5.
- [10] M. J. Dugan, H. Georgi, and D. B. Kaplan, "Anatomy of a composite Higgs model", *Nucl. Phys. B* **254** (1985) 299, doi:10.1016/0550-3213(85)90221-4.
- [11] J. A. Aguilar-Saavedra, "Mixing with vector-like quarks: constraints and expectations", in *LHCP 2013 – Large Hadron Collider Physics 2013*, p. 16012. 2013. arXiv:1306.4432. doi:10.1051/epjconf/20136016012.
- [12] F. del Aguila, J. A. Aguilar-Saavedra, and R. Miquel, "Constraints on top couplings in models with exotic quarks", *Phys. Rev. Lett.* **82** (1999) 1628, doi:10.1103/PhysRevLett.82.1628, arXiv:hep-ph/9808400.
- [13] ALEPH, LEP Electroweak, L3, DELPHI, and OPAL Collaborations, "Electroweak measurements in electron-positron collisions at W-boson-pair energies at LEP", *Phys. Rept.* **532** (2013) 119, doi:10.1016/j.physrep.2013.07.004, arXiv:1302.3415.
- [14] O. Eberhardt et al., "Impact of a Higgs boson at a mass of 126 GeV on the standard model with three and four fermion generations", *Phys. Rev. Lett.* **109** (2012) 241802, doi:10.1103/PhysRevLett.109.241802, arXiv:1209.1101.

- [15] A. Djouadi and A. Lenz, “Sealing the fate of a fourth generation of fermions”, *Phys. Lett. B* **715** (2012) 310, doi:10.1016/j.physletb.2012.07.060, arXiv:1204.1252.
- [16] J. A. Aguilar-Saavedra, R. Benbrik, S. Heinemeyer, and M. Pérez-Victoria, “Handbook of vectorlike quarks: Mixing and single production”, *Phys. Rev. D* **88** (2013) 094010, doi:10.1103/PhysRevD.88.094010.
- [17] J. Ellis, “TikZ-Feynman: Feynman diagrams with TikZ”, *Comput. Phys. Commun.* **210** (2017) 103, doi:10.1016/j.cpc.2016.08.019, arXiv:1601.05437.
- [18] A. De Simone, O. Matsedonskyi, R. Rattazzi, and A. Wulzer, “A first top partner hunter’s guide”, *JHEP* **04** (2013) 004, doi:10.1007/JHEP04(2013)004, arXiv:1211.5663.
- [19] F. del Aguila, L. Ametller, G. L. Kane, and J. Vidal, “Vector like fermion and standard Higgs production at hadron colliders”, *Nucl. Phys. B* **334** (1990) 1, doi:10.1016/0550-3213(90)90655-W.
- [20] O. Matsedonskyi, G. Panico, and A. Wulzer, “On the interpretation of top partners searches”, *JHEP* **12** (2014) 097, doi:10.1007/JHEP12(2014)097, arXiv:1409.0100.
- [21] CMS Collaboration, “Search for vector-like charge $2/3$ T quarks in proton-proton collisions at $\sqrt{s} = 8$ TeV”, *Phys. Rev. D* **93** (2016) 012003, doi:10.1103/PhysRevD.92.012003, arXiv:1509.04177.
- [22] CMS Collaboration, “Inclusive search for a vector-like T quark with charge $\frac{2}{3}$ in pp collisions at $\sqrt{s} = 8$ TeV”, *Phys. Lett. B* **729** (2014) 149, doi:10.1016/j.physletb.2014.01.006, arXiv:1311.7667.
- [23] ATLAS Collaboration, “Search for pair production of a new heavy quark that decays into a w boson and a light quark in pp collisions at $\sqrt{s} = 8$ TeV with the atlas detector”, *Phys. Rev. D* **92** (2015) 112007, doi:10.1103/PhysRevD.92.112007, arXiv:1509.04261.
- [24] ATLAS Collaboration, “Search for production of vector-like quark pairs and of four top quarks in the lepton-plus-jets final state in pp collisions at $\sqrt{s} = 8$ TeV with the atlas detector”, *JHEP* **08** (2015) 105, doi:10.1007/JHEP08(2015)105, arXiv:1505.04306.
- [25] CMS Collaboration, “Search for pair-produced vectorlike B quarks in proton-proton collisions at $\sqrt{s} = 8$ TeV”, *Phys. Rev. D* **93** (2016) 112009, doi:10.1103/PhysRevD.93.112009, arXiv:1507.07129.
- [26] ATLAS Collaboration, “Search for vector-like B quarks in events with one isolated lepton, missing transverse momentum and jets at $\sqrt{s} = 8$ TeV with the ATLAS detector”, *Phys. Rev. D* **91** (2015) 112011, doi:10.1103/PhysRevD.91.112011, arXiv:1503.05425.
- [27] ATLAS Collaboration, “Search for pair production of vector-like top quarks in events with one lepton, jets, and missing transverse momentum in $\sqrt{s} = 13$ TeV pp collisions with the ATLAS detector”, (2017). arXiv:1705.10751. Submitted to JHEP.
- [28] ATLAS Collaboration, “Search for pair production of heavy vector-like quarks decaying to high- p_T W bosons and b quarks in the lepton-plus-jets final state in pp collisions at $\sqrt{s}=13$ TeV with the ATLAS detector”, (2017). arXiv:1707.03347. Submitted to JHEP.

- [29] CMS Collaboration, “The CMS experiment at the CERN LHC”, *JINST* **3** (2008) S08004, doi:10.1088/1748-0221/3/08/S08004.
- [30] CMS Collaboration, “Particle-flow reconstruction and global event description with the CMS detector”, (2017). arXiv:1706.04965. Submitted to JINST.
- [31] CMS Collaboration, “Performance of electron reconstruction and selection with the CMS detector in proton-proton collisions at $\sqrt{s} = 8$ TeV”, *JINST* **10** (2015) P06005, doi:10.1088/1748-0221/10/06/P06005, arXiv:1502.02701.
- [32] CMS Collaboration, “Performance of CMS muon reconstruction in pp collision events at $\sqrt{s} = 7$ TeV”, *JINST* **7** (2012) P10002, doi:10.1088/1748-0221/7/10/P10002, arXiv:1206.4071.
- [33] M. Cacciari, G. P. Salam, and G. Soyez, “The anti- k_t jet clustering algorithm”, *JHEP* **04** (2008) 063, doi:10.1088/1126-6708/2008/04/063, arXiv:0802.1189.
- [34] M. Cacciari, G. P. Salam, and G. Soyez, “FastJet user manual”, *Eur. Phys. J. C* **72** (2012) 1896, doi:10.1140/epjc/s10052-012-1896-2, arXiv:1111.6097.
- [35] M. Cacciari, G. P. Salam, and G. Soyez, “The catchment area of jets”, *JHEP* **04** (2008) 005, doi:10.1088/1126-6708/2008/04/005, arXiv:0802.1188.
- [36] CMS Collaboration, “Jet energy scale and resolution in the CMS experiment in pp collisions at 8 TeV”, *JINST* **12** (2017) P02014, doi:10.1088/1748-0221/12/02/P02014, arXiv:1607.03663.
- [37] CMS Collaboration, “Determination of jet energy calibration and transverse momentum resolution in CMS”, *JINST* **6** (2011) P11002, doi:10.1088/1748-0221/6/11/P11002, arXiv:1107.4277.
- [38] P. Nason, “A new method for combining NLO QCD with shower Monte Carlo algorithms”, *JHEP* **11** (2004) 040, doi:10.1088/1126-6708/2004/11/040, arXiv:hep-ph/0409146.
- [39] S. Frixione, P. Nason, and C. Oleari, “Matching NLO QCD computations with parton shower simulations: the POWHEG method”, *JHEP* **11** (2007) 070, doi:10.1088/1126-6708/2007/11/070, arXiv:0709.2092.
- [40] S. Alioli, P. Nason, C. Oleari, and E. Re, “A general framework for implementing NLO calculations in shower Monte Carlo programs: the POWHEG BOX”, *JHEP* **06** (2010) 043, doi:10.1007/JHEP06(2010)043, arXiv:1002.2581.
- [41] S. Frixione, P. Nason, and G. Ridolfi, “A positive-weight next-to-leading-order Monte Carlo for heavy flavour hadroproduction”, *JHEP* **09** (2007) 126, doi:10.1088/1126-6708/2007/09/126, arXiv:0707.3088.
- [42] J. Alwall et al., “The automated computation of tree-level and next-to-leading order differential cross sections, and their matching to parton shower simulations”, *JHEP* **07** (2014) 079, doi:10.1007/JHEP07(2014)079, arXiv:hep-ph/1405.0301.
- [43] R. Frederix and S. Frixione, “Merging meets matching in MC@NLO”, *JHEP* **12** (2012) 061, doi:10.1007/JHEP12(2012)061, arXiv:1209.6215.

- [44] J. Alwall et al., “Comparative study of various algorithms for the merging of parton showers and matrix elements in hadronic collisions”, *Eur. Phys. J. C* **53** (2008) 473, doi:10.1140/epjc/s10052-007-0490-5, arXiv:0706.2569.
- [45] T. Sjöstrand, S. Mrenna and P. Skands, “PYTHIA 6.4 physics and manual”, *JHEP* **05** (2006) 026, doi:10.1088/1126-6708/2006/05/026, arXiv:hep-ph/0603175.
- [46] T. Sjöstrand et al., “An introduction to pythia 8.2”, *Comput. Phys. Commun.* **191** (2015) 159, doi:10.1016/j.cpc.2015.01.024, arXiv:1410.3012.
- [47] M. Czakon and A. Mitov, “Top++: A program for the calculation of the top-pair cross-section at hadron colliders”, *Comput. Phys. Commun.* **185** (2014) 2930, doi:10.1016/j.cpc.2014.06.021, arXiv:1112.5675.
- [48] M. Czakon, P. Fiedler, and A. Mitov, “Total top-quark pair-production cross section at hadron colliders through $\mathcal{O}(\alpha_s^4)$ ”, *Phys. Rev. Lett.* **110** (2013) 252004, doi:10.1103/PhysRevLett.110.252004, arXiv:1303.6254.
- [49] M. Czakon and A. Mitov, “NNLO corrections to top pair production at hadron colliders: the quark-gluon reaction”, *JHEP* **01** (2013) 080, doi:10.1007/JHEP01(2013)080, arXiv:1210.6832.
- [50] M. Czakon and A. Mitov, “NNLO corrections to top-pair production at hadron colliders: the all-fermionic scattering channels”, *JHEP* **12** (2012) 054, doi:10.1007/JHEP12(2012)054, arXiv:1207.0236.
- [51] P. Bärnreuther, M. Czakon, and A. Mitov, “Percent level precision physics at the Tevatron: First genuine NNLO QCD corrections to $q\bar{q} \rightarrow t\bar{t} + x$ ”, *Phys. Rev. Lett.* **109** (2012) 132001, doi:10.1103/PhysRevLett.109.132001, arXiv:1204.5201.
- [52] M. Cacciari et al., “Top-pair production at hadron colliders with next-to-next-to-leading logarithmic soft-gluon resummation”, *Phys. Lett. B* **710** (2012) 612, doi:10.1016/j.physletb.2012.03.013, arXiv:1111.5869.
- [53] P. Skands, S. Carrazza, and J. Rojo, “Tuning PYTHIA 8.1: the Monash 2013 tune”, *Eur. Phys. J. C* **74** (2014) 3024, doi:10.1140/epjc/s10052-014-3024-y, arXiv:1404.5630.
- [54] CMS Collaboration, “Event generator tunes obtained from underlying event and multiparton scattering measurements”, *Eur. Phys. J. C* **76** (2016) 155, doi:10.1140/epjc/s10052-016-3988-x, arXiv:1512.00815.
- [55] NNPDF Collaboration, “Parton distributions for the LHC Run II”, *JHEP* **04** (2015) 040, doi:10.1007/JHEP04(2015)040, arXiv:1410.8849.
- [56] GEANT4 Collaboration, “GEANT4: A simulation toolkit”, *Nucl. Instrum. Meth. A* **506** (2003) 250, doi:10.1016/S0168-9002(03)01368-8.
- [57] CMS Collaboration, “Description and performance of track and primary-vertex reconstruction with the CMS tracker”, *JINST* **9** (2014) P10009, doi:10.1088/1748-0221/9/10/P10009, arXiv:1405.6569.
- [58] ATLAS Collaboration, “Measurement of the inelastic proton-proton cross section at $\sqrt{s} = 13$ TeV with the ATLAS detector at the LHC”, *Phys. Rev. Lett.* **117** (2016) 182002, doi:10.1103/PhysRevLett.117.182002, arXiv:1606.02625.

- [59] CMS Collaboration, “Measurements of inclusive W and Z cross sections in pp collisions at $\sqrt{s} = 7$ TeV”, *JHEP* **01** (2011) 080, doi:10.1007/JHEP01(2011)080, arXiv:1012.2466.
- [60] J. Thaler and K. Van Tilburg, “Maximizing boosted top identification by minimizing N-subjettiness”, *JHEP* **02** (2012) 093, doi:10.1007/JHEP02(2012)093, arXiv:1108.2701.
- [61] S. D. Ellis, C. K. Vermilion, and J. R. Walsh, “Techniques for improved heavy particle searches with jet substructure”, *Phys. Rev. D* **80** (2009) 051501, doi:10.1103/PhysRevD.80.051501, arXiv:0903.5081.
- [62] A. J. Larkoski, S. Marzani, G. Soyez, and J. Thaler, “Soft drop”, *JHEP* **05** (2014) 146, doi:10.1007/JHEP05(2014)146, arXiv:hep-ph/1402.2657.
- [63] CMS Collaboration, “Identification of b-quark jets with the CMS experiment”, *JINST* **8** (2013) P04013, doi:10.1088/1748-0221/8/04/P04013, arXiv:1211.4462.
- [64] CMS Collaboration, “Jet algorithms performance in 13 TeV data”, CMS Physics Analysis Summary CMS-PAS-JME-16-003, 2016.
- [65] CMS Collaboration, “Search for electroweak production of a vector-like quark decaying to a top quark and a Higgs boson using boosted topologies in fully hadronic final states”, *JHEP* **04** (2017) 136, doi:10.1007/JHEP04(2017)136, arXiv:1612.05336.
- [66] CMS Collaboration, “Search for single production of vector-like quarks decaying into a b quark and a W boson in proton-proton collisions at $\sqrt{s} = 13$ TeV”, (2017). arXiv:1701.08328. Submitted to Phys. Lett. B.
- [67] G. Cowan, “PDG review on statistics (chap. 39)”, *Chin. Phys. C* **40** (2016) 100001, doi:10.1088/1674-1137/40/10/100001.
- [68] T. Müller, J. Ott, and J. Wagner-Kuhr, “theta – a framework for template-based modeling and inference”, 2012. <http://www-ekp.physik.uni-karlsruhe.de/~ott/theta/theta-auto/index.html>.
- [69] CMS Collaboration, “CMS luminosity measurement for the 2015 data-taking period”, Technical Report CMS-PAS-LUM-15-001, 2017.
- [70] CMS Collaboration, “Measurement of the ZZ production cross section and Z $\rightarrow \ell^+ \ell^- \ell'^+ \ell'^-$ branching fraction in pp collisions at $\sqrt{s} = 13$ TeV”, *Phys. Lett. B* **763** (2016) 280, doi:10.1016/j.physletb.2016.10.054, arXiv:1607.08834.
- [71] CMS Collaboration, “Measurement of the WZ production cross section in pp collisions at $\sqrt{s} = 13$ TeV”, *Phys. Lett. B* **766** (2017) 268, doi:10.1016/j.physletb.2017.01.011, arXiv:1607.06943.
- [72] M. Bähr et al., “Herwig++ physics and manual”, *Eur. Phys. J. C* **58** (2008) 639, doi:10.1140/epjc/s10052-008-0798-9, arXiv:0803.0883.
- [73] R. J. Barlow and C. Beeston, “Fitting using finite monte carlo samples”, *Comput. Phys. Commun.* (1993) 219, doi:10.1016/0010-4655(93)90005-W.

A The CMS Collaboration

Yerevan Physics Institute, Yerevan, Armenia

A.M. Sirunyan, A. Tumasyan

Institut für Hochenergiephysik, Wien, Austria

W. Adam, F. Ambrogio, E. Asilar, T. Bergauer, J. Brandstetter, E. Brondolin, M. Dragicevic, J. Erö, M. Flechl, M. Friedl, R. Frühwirth¹, V.M. Ghete, J. Grossmann, J. Hrubec, M. Jeitler¹, A. König, N. Krammer, I. Krätschmer, D. Liko, T. Madlener, I. Mikulec, E. Pree, D. Rabady, N. Rad, H. Rohringer, J. Schieck¹, R. Schöfbeck, M. Spanring, D. Spitzbart, J. Strauss, W. Waltenberger, J. Wittmann, C.-E. Wulz¹, M. Zarucki

Institute for Nuclear Problems, Minsk, Belarus

V. Chekhovsky, V. Mossolov, J. Suarez Gonzalez

Universiteit Antwerpen, Antwerpen, Belgium

E.A. De Wolf, D. Di Croce, X. Janssen, J. Lauwers, M. Van De Klundert, H. Van Haeveermaet, P. Van Mechelen, N. Van Remortel, A. Van Spilbeeck

Vrije Universiteit Brussel, Brussel, Belgium

S. Abu Zeid, F. Blekman, J. D'Hondt, I. De Bruyn, J. De Clercq, K. Deroover, G. Flouris, D. Lontkovskyi, S. Lowette, S. Moortgat, L. Moreels, A. Olbrechts, Q. Python, K. Skovpen, S. Tavernier, W. Van Doninck, P. Van Mulders, I. Van Parijs

Université Libre de Bruxelles, Bruxelles, Belgium

H. Brun, B. Clerboux, G. De Lentdecker, H. Delannoy, G. Fasanella, L. Favart, R. Goldouzian, A. Grebenyuk, G. Karapostoli, T. Lenzi, J. Luetic, T. Maerschalk, A. Marinov, A. Randle-conde, T. Seva, C. Vander Velde, P. Vanlaer, D. Vannerom, R. Yonamine, F. Zenoni, F. Zhang²

Ghent University, Ghent, Belgium

A. Cimmino, T. Cornelis, D. Dobur, A. Fagot, M. Gul, I. Khvastunov, D. Poyraz, C. Roskas, S. Salva, M. Tytgat, W. Verbeke, N. Zaganidis

Université Catholique de Louvain, Louvain-la-Neuve, Belgium

H. Bakhshiansohi, O. Bondu, S. Brochet, G. Bruno, A. Caudron, S. De Visscher, C. Delaere, M. Delcourt, B. Francois, A. Giammanco, A. Jafari, M. Komm, G. Krintiras, V. Lemaitre, A. Magitteri, A. Mertens, M. Musich, K. Piotrkowski, L. Quertenmont, M. Vidal Marono, S. Wertz

Université de Mons, Mons, Belgium

N. Bely

Centro Brasileiro de Pesquisas Fisicas, Rio de Janeiro, Brazil

W.L. Aldá Júnior, F.L. Alves, G.A. Alves, L. Brito, M. Correa Martins Junior, C. Hensel, A. Moraes, M.E. Pol, P. Rebello Teles

Universidade do Estado do Rio de Janeiro, Rio de Janeiro, Brazil

E. Belchior Batista Das Chagas, W. Carvalho, J. Chinellato³, A. Custódio, E.M. Da Costa, G.G. Da Silveira⁴, D. De Jesus Damiao, S. Fonseca De Souza, L.M. Huertas Guativa, H. Malbouisson, M. Melo De Almeida, C. Mora Herrera, L. Mundim, H. Nogima, A. Santoro, A. Sznajder, E.J. Tonelli Manganote³, F. Torres Da Silva De Araujo, A. Vilela Pereira

Universidade Estadual Paulista ^a, Universidade Federal do ABC ^b, São Paulo, Brazil

S. Ahuja^a, C.A. Bernardes^a, T.R. Fernandez Perez Tomei^a, E.M. Gregores^b, P.G. Mercadante^b, C.S. Moon^a, S.F. Novaes^a, Sandra S. Padula^a, D. Romero Abad^b, J.C. Ruiz Vargas^a

Institute for Nuclear Research and Nuclear Energy of Bulgaria Academy of Sciences

A. Aleksandrov, R. Hadjiiska, P. Iaydjiev, M. Misheva, M. Rodozov, M. Shopova, S. Stoykova, G. Sultanov

University of Sofia, Sofia, Bulgaria

A. Dimitrov, I. Glushkov, L. Litov, B. Pavlov, P. Petkov

Beihang University, Beijing, China

W. Fang⁵, X. Gao⁵

Institute of High Energy Physics, Beijing, China

M. Ahmad, J.G. Bian, G.M. Chen, H.S. Chen, M. Chen, Y. Chen, C.H. Jiang, D. Leggat, Z. Liu, F. Romeo, S.M. Shaheen, A. Spiezia, J. Tao, C. Wang, Z. Wang, E. Yazgan, H. Zhang, J. Zhao

State Key Laboratory of Nuclear Physics and Technology, Peking University, Beijing, China

Y. Ban, G. Chen, Q. Li, S. Liu, Y. Mao, S.J. Qian, D. Wang, Z. Xu

Universidad de Los Andes, Bogota, Colombia

C. Avila, A. Cabrera, L.F. Chaparro Sierra, C. Florez, C.F. González Hernández, J.D. Ruiz Alvarez

University of Split, Faculty of Electrical Engineering, Mechanical Engineering and Naval Architecture, Split, Croatia

B. Courbon, N. Godinovic, D. Lelas, I. Puljak, P.M. Ribeiro Cipriano, T. Sculac

University of Split, Faculty of Science, Split, Croatia

Z. Antunovic, M. Kovac

Institute Rudjer Boskovic, Zagreb, Croatia

V. Brigljevic, D. Ferencek, K. Kadija, B. Mesic, T. Susa

University of Cyprus, Nicosia, Cyprus

M.W. Ather, A. Attikis, G. Mavromanolakis, J. Mousa, C. Nicolaou, F. Ptochos, P.A. Razis, H. Rykaczewski

Charles University, Prague, Czech Republic

M. Finger⁶, M. Finger Jr.⁶

Universidad San Francisco de Quito, Quito, Ecuador

E. Carrera Jarrin

Academy of Scientific Research and Technology of the Arab Republic of Egypt, Egyptian Network of High Energy Physics, Cairo, Egypt

A.A. Abdelalim^{7,8}, Y. Mohammed⁹, E. Salama^{10,11}

National Institute of Chemical Physics and Biophysics, Tallinn, Estonia

R.K. Dewanjee, M. Kadastik, L. Perrini, M. Raidal, A. Tiko, C. Veelken

Department of Physics, University of Helsinki, Helsinki, Finland

P. Eerola, J. Pekkanen, M. Voutilainen

Helsinki Institute of Physics, Helsinki, Finland

J. Härkönen, T. Järvinen, V. Karimäki, R. Kinnunen, T. Lampén, K. Lassila-Perini, S. Lehti, T. Lindén, P. Luukka, E. Tuominen, J. Tuominiemi, E. Tuovinen

Lappeenranta University of Technology, Lappeenranta, Finland

J. Talvitie, T. Tuuva

IRFU, CEA, Université Paris-Saclay, Gif-sur-Yvette, France

M. Besancon, F. Couderc, M. Dejardin, D. Denegri, J.L. Faure, F. Ferri, S. Ganjour, S. Ghosh, A. Givernaud, P. Gras, G. Hamel de Monchenault, P. Jarry, I. Kucher, E. Locci, M. Machet, J. Malcles, G. Negro, J. Rander, A. Rosowsky, M.Ö. Sahin, M. Titov

Laboratoire Leprince-Ringuet, Ecole polytechnique, CNRS/IN2P3, Université Paris-Saclay, Palaiseau, France

A. Abdulsalam, I. Antropov, S. Baffioni, F. Beaudette, P. Busson, L. Cadamuro, C. Charlot, O. Davignon, R. Granier de Cassagnac, M. Jo, S. Lisniak, A. Lobanov, J. Martin Blanco, M. Nguyen, C. Ochando, G. Ortona, P. Paganini, P. Pigard, S. Regnard, R. Salerno, J.B. Sauvan, Y. Sirois, A.G. Stahl Leitner, T. Strebler, Y. Yilmaz, A. Zabi, A. Zghiche

Université de Strasbourg, CNRS, IPHC UMR 7178, F-67000 Strasbourg, France

J.-L. Agram¹², J. Andrea, D. Bloch, J.-M. Brom, M. Buttignol, E.C. Chabert, N. Chanon, C. Collard, E. Conte¹², X. Coubez, J.-C. Fontaine¹², D. Gelé, U. Goerlach, M. Jansová, A.-C. Le Bihan, P. Van Hove

Centre de Calcul de l'Institut National de Physique Nucleaire et de Physique des Particules, CNRS/IN2P3, Villeurbanne, France

S. Gadrat

Université de Lyon, Université Claude Bernard Lyon 1, CNRS-IN2P3, Institut de Physique Nucléaire de Lyon, Villeurbanne, France

S. Beauceron, C. Bernet, G. Boudoul, R. Chierici, D. Contardo, P. Depasse, H. El Mamouni, J. Fay, L. Finco, S. Gascon, M. Gouzevitch, G. Grenier, B. Ille, F. Lagarde, I.B. Laktineh, M. Lethuillier, L. Mirabito, A.L. Pequegnot, S. Perries, A. Popov¹³, V. Sordini, M. Vander Donckt, S. Viret

Georgian Technical University, Tbilisi, Georgia

A. Khvedelidze⁶

Tbilisi State University, Tbilisi, Georgia

I. Bagaturia¹⁴

RWTH Aachen University, I. Physikalisches Institut, Aachen, Germany

C. Autermann, S. Beranek, L. Feld, M.K. Kiesel, K. Klein, M. Lipinski, M. Preuten, C. Schomakers, J. Schulz, T. Verlage

RWTH Aachen University, III. Physikalisches Institut A, Aachen, Germany

A. Albert, M. Brodski, E. Dietz-Laursonn, D. Duchardt, M. Endres, M. Erdmann, S. Erdweg, T. Esch, R. Fischer, A. Güth, M. Hamer, T. Hebbeker, C. Heidemann, K. Hoepfner, S. Knutzen, M. Merschmeyer, A. Meyer, P. Millet, S. Mukherjee, M. Olschewski, K. Padeken, T. Pook, M. Radziej, H. Reithler, M. Rieger, F. Scheuch, D. Teyssier, S. Thüer

RWTH Aachen University, III. Physikalisches Institut B, Aachen, Germany

G. Flügge, B. Kargoll, T. Kress, A. Künsken, J. Lingemann, T. Müller, A. Nehr Korn, A. Nowack, C. Pistone, O. Pooth, A. Stahl¹⁵

Deutsches Elektronen-Synchrotron, Hamburg, Germany

M. Aldaya Martin, T. Arndt, C. Asawatangkuldee, K. Beernaert, O. Behnke, U. Behrens, A.A. Bin Anuar, K. Borras¹⁶, V. Botta, A. Campbell, P. Connor, C. Contreras-Campana, F. Costanza, C. Diez Pardos, G. Eckerlin, D. Eckstein, T. Eichhorn, E. Eren, E. Gallo¹⁷, J. Garay Garcia, A. Geiser, A. Gizhko, J.M. Grados Luyando, A. Grohsjean, P. Gunnellini, A. Harb, J. Hauk, M. Hempel¹⁸, H. Jung, A. Kalogeropoulos, M. Kasemann, J. Keaveney, C. Kleinwort,

I. Korol, D. Krücker, W. Lange, A. Lelek, T. Lenz, J. Leonard, K. Lipka, W. Lohmann¹⁸, R. Mankel, I.-A. Melzer-Pellmann, A.B. Meyer, G. Mittag, J. Mnich, A. Mussgiller, E. Ntomari, D. Pitzl, R. Placakyte, A. Raspereza, B. Roland, M. Savitskyi, P. Saxena, R. Shevchenko, S. Spannagel, N. Stefaniuk, G.P. Van Onsem, R. Walsh, Y. Wen, K. Wichmann, C. Wissing, O. Zenaiev

University of Hamburg, Hamburg, Germany

S. Bein, V. Blobel, M. Centis Vignali, A.R. Draeger, T. Dreyer, E. Garutti, D. Gonzalez, J. Haller, M. Hoffmann, A. Junkes, A. Karavdina, R. Klanner, R. Kogler, N. Kovalchuk, S. Kurz, T. Lapsien, I. Marchesini, D. Marconi, M. Meyer, M. Niedziela, D. Nowatschin, F. Pantaleo¹⁵, T. Peiffer, A. Perieanu, C. Scharf, P. Schleper, A. Schmidt, S. Schumann, J. Schwandt, J. Sonneveld, H. Stadie, G. Steinbrück, F.M. Stober, M. Stöver, H. Tholen, D. Troendle, E. Usai, L. Vanelderden, A. Vanhoefer, B. Vormwald

Institut für Experimentelle Kernphysik, Karlsruhe, Germany

M. Akbiyik, C. Barth, S. Baur, E. Butz, R. Caspart, T. Chwalek, F. Colombo, W. De Boer, A. Dierlamm, B. Freund, R. Friese, M. Giffels, A. Gilbert, D. Haitz, F. Hartmann¹⁵, S.M. Heindl, U. Husemann, F. Kassel¹⁵, S. Kudella, H. Mildner, M.U. Mozer, Th. Müller, M. Plagge, G. Quast, K. Rabbertz, M. Schröder, I. Shvetsov, G. Sieber, H.J. Simonis, R. Ulrich, S. Wayand, M. Weber, T. Weiler, S. Williamson, C. Wöhrmann, R. Wolf

Institute of Nuclear and Particle Physics (INPP), NCSR Demokritos, Aghia Paraskevi, Greece

G. Anagnostou, G. Daskalakis, T. Geralis, V.A. Giakoumopoulou, A. Kyriakis, D. Loukas, I. Topsis-Giotis

National and Kapodistrian University of Athens, Athens, Greece

S. Kesisoglou, A. Panagiotou, N. Saoulidou

University of Ioánnina, Ioánnina, Greece

I. Evangelou, C. Foudas, P. Kokkas, N. Manthos, I. Papadopoulos, E. Paradas, J. Strologas, F.A. Triantis

MTA-ELTE Lendület CMS Particle and Nuclear Physics Group, Eötvös Loránd University, Budapest, Hungary

M. Csanad, N. Filipovic, G. Pasztor

Wigner Research Centre for Physics, Budapest, Hungary

G. Bencze, C. Hajdu, D. Horvath¹⁹, Á. Hunyadi, F. Sikler, V. Veszpremi, G. Vesztergombi²⁰, A.J. Zsigmond

Institute of Nuclear Research ATOMKI, Debrecen, Hungary

N. Beni, S. Czellar, J. Karancsi²¹, A. Makovec, J. Molnar, Z. Szillasi

Institute of Physics, University of Debrecen, Debrecen, Hungary

M. Bartók²⁰, P. Raics, Z.L. Trocsanyi, B. Ujvari

Indian Institute of Science (IISc), Bangalore, India

S. Choudhury, J.R. Komaragiri

National Institute of Science Education and Research, Bhubaneswar, India

S. Bahinipati²², S. Bhowmik, P. Mal, K. Mandal, A. Nayak²³, D.K. Sahoo²², N. Sahoo, S.K. Swain

Panjab University, Chandigarh, India

S. Bansal, S.B. Beri, V. Bhatnagar, U. Bhawandeep, R. Chawla, N. Dhingra, A.K. Kalsi, A. Kaur, M. Kaur, R. Kumar, P. Kumari, A. Mehta, J.B. Singh, G. Walia

University of Delhi, Delhi, India

Ashok Kumar, Aashaq Shah, A. Bhardwaj, S. Chauhan, B.C. Choudhary, R.B. Garg, S. Keshri, A. Kumar, S. Malhotra, M. Naimuddin, K. Ranjan, R. Sharma, V. Sharma

Saha Institute of Nuclear Physics, HBNI, Kolkata, India

R. Bhardwaj, R. Bhattacharya, S. Bhattacharya, S. Dey, S. Dutt, S. Dutta, S. Ghosh, N. Majumdar, A. Modak, K. Mondal, S. Mukhopadhyay, S. Nandan, A. Purohit, A. Roy, D. Roy, S. Roy Chowdhury, S. Sarkar, M. Sharan, S. Thakur

Indian Institute of Technology Madras, Madras, India

P.K. Behera

Bhabha Atomic Research Centre, Mumbai, India

R. Chudasama, D. Dutta, V. Jha, V. Kumar, A.K. Mohanty¹⁵, P.K. Netrakanti, L.M. Pant, P. Shukla, A. Topkar

Tata Institute of Fundamental Research-A, Mumbai, India

T. Aziz, S. Dugad, B. Mahakud, S. Mitra, G.B. Mohanty, B. Parida, N. Sur, B. Sutar

Tata Institute of Fundamental Research-B, Mumbai, India

S. Banerjee, S. Bhattacharya, S. Chatterjee, P. Das, M. Guchait, Sa. Jain, S. Kumar, M. Maity²⁴, G. Majumder, K. Mazumdar, T. Sarkar²⁴, N. Wickramage²⁵

Indian Institute of Science Education and Research (IISER), Pune, India

S. Chauhan, S. Dube, V. Hegde, A. Kapoor, K. Kothekar, S. Pandey, A. Rane, S. Sharma

Institute for Research in Fundamental Sciences (IPM), Tehran, Iran

S. Chenarani²⁶, E. Eskandari Tadavani, S.M. Etesami²⁶, M. Khakzad, M. Mohammadi Najafabadi, M. Naseri, S. Paktinat Mehdiabadi²⁷, F. Rezaei Hosseinabadi, B. Safarzadeh²⁸, M. Zeinali

University College Dublin, Dublin, Ireland

M. Felcini, M. Grunewald

INFN Sezione di Bari ^a, Università di Bari ^b, Politecnico di Bari ^c, Bari, Italy

M. Abbrescia^{a,b}, C. Calabria^{a,b}, C. Caputo^{a,b}, A. Colaleo^a, D. Creanza^{a,c}, L. Cristella^{a,b}, N. De Filippis^{a,c}, M. De Palma^{a,b}, F. Errico^{a,b}, L. Fiore^a, G. Iaselli^{a,c}, G. Maggi^{a,c}, M. Maggi^a, G. Miniello^{a,b}, S. My^{a,b}, S. Nuzzo^{a,b}, A. Pompili^{a,b}, G. Pugliese^{a,c}, R. Radogna^{a,b}, A. Ranieri^a, G. Selvaggi^{a,b}, A. Sharma^a, L. Silvestris^{a,15}, R. Venditti^a, P. Verwilligen^a

INFN Sezione di Bologna ^a, Università di Bologna ^b, Bologna, Italy

G. Abbiendi^a, C. Battilana, D. Bonacorsi^{a,b}, S. Braibant-Giacomelli^{a,b}, L. Brigliadori^{a,b}, R. Campanini^{a,b}, P. Capiluppi^{a,b}, A. Castro^{a,b}, F.R. Cavallo^a, S.S. Chhibra^{a,b}, G. Codispoti^{a,b}, M. Cuffiani^{a,b}, G.M. Dallavalle^a, F. Fabbri^a, A. Fanfani^{a,b}, D. Fasanella^{a,b}, P. Giacomelli^a, L. Guiducci^{a,b}, S. Marcellini^a, G. Masetti^a, F.L. Navarria^{a,b}, A. Perrotta^a, A.M. Rossi^{a,b}, T. Rovelli^{a,b}, G.P. Siroli^{a,b}, N. Tosi^{a,b,15}

INFN Sezione di Catania ^a, Università di Catania ^b, Catania, Italy

S. Albergo^{a,b}, S. Costa^{a,b}, A. Di Mattia^a, F. Giordano^{a,b}, R. Potenza^{a,b}, A. Tricomi^{a,b}, C. Tuve^{a,b}

INFN Sezione di Firenze ^a, Università di Firenze ^b, Firenze, Italy

G. Barbagli^a, K. Chatterjee^{a,b}, V. Ciulli^{a,b}, C. Civinini^a, R. D'Alessandro^{a,b}, E. Focardi^{a,b}, P. Lenzi^{a,b}, M. Meschini^a, S. Paoletti^a, L. Russo^{a,29}, G. Sguazzoni^a, D. Strom^a, L. Viliani^{a,b,15}

INFN Laboratori Nazionali di Frascati, Frascati, Italy

L. Benussi, S. Bianco, F. Fabbri, D. Piccolo, F. Primavera¹⁵

INFN Sezione di Genova ^a, Università di Genova ^b, Genova, Italy

V. Calvelli^{a,b}, F. Ferro^a, E. Robutti^a, S. Tosi^{a,b}

INFN Sezione di Milano-Bicocca ^a, Università di Milano-Bicocca ^b, Milano, Italy

L. Brianza^{a,b}, F. Brivio^{a,b}, V. Ciriolo^{a,b}, M.E. Dinardo^{a,b}, S. Fiorendi^{a,b}, S. Gennai^a, A. Ghezzi^{a,b}, P. Govoni^{a,b}, M. Malberti^{a,b}, S. Malvezzi^a, R.A. Manzoni^{a,b}, D. Menasce^a, L. Moroni^a, M. Paganoni^{a,b}, K. Pauwels^{a,b}, D. Pedrini^a, S. Pigazzini^{a,b,30}, S. Ragazzi^{a,b}, T. Tabarelli de Fatis^{a,b}

INFN Sezione di Napoli ^a, Università di Napoli 'Federico II' ^b, Napoli, Italy, Università della Basilicata ^c, Potenza, Italy, Università G. Marconi ^d, Roma, Italy

S. Buontempo^a, N. Cavallo^{a,c}, S. Di Guida^{a,d,15}, F. Fabozzi^{a,c}, F. Fienga^{a,b}, A.O.M. Iorio^{a,b}, W.A. Khan^a, L. Lista^a, S. Meola^{a,d,15}, P. Paolucci^{a,15}, C. Sciacca^{a,b}, F. Thyssen^a

INFN Sezione di Padova ^a, Università di Padova ^b, Padova, Italy, Università di Trento ^c, Trento, Italy

P. Azzi^{a,15}, N. Bacchetta^a, L. Benato^{a,b}, A. Boletti^{a,b}, R. Carlin^{a,b}, A. Carvalho Antunes De Oliveira^{a,b}, P. Checchia^a, M. Dall'Osso^{a,b}, P. De Castro Manzano^a, T. Dorigo^a, U. Dosselli^a, U. Gasparini^{a,b}, A. Gozzelino^a, S. Lacaprara^a, M. Margoni^{a,b}, A.T. Meneguzzo^{a,b}, N. Pozzobon^{a,b}, P. Ronchese^{a,b}, R. Rossin^{a,b}, M. Sgaravatto^a, F. Simonetto^{a,b}, E. Torassa^a, S. Ventura^a, M. Zanetti^{a,b}, P. Zotto^{a,b}, G. Zumerle^{a,b}

INFN Sezione di Pavia ^a, Università di Pavia ^b, Pavia, Italy

A. Braghieri^a, F. Fallavollita^{a,b}, A. Magnani^{a,b}, P. Montagna^{a,b}, S.P. Ratti^{a,b}, V. Re^a, M. Ressegotti, C. Riccardi^{a,b}, P. Salvini^a, I. Vai^{a,b}, P. Vitulo^{a,b}

INFN Sezione di Perugia ^a, Università di Perugia ^b, Perugia, Italy

L. Alunni Solestizi^{a,b}, G.M. Bilei^a, D. Ciangottini^{a,b}, L. Fanò^{a,b}, P. Lariccia^{a,b}, R. Leonardi^{a,b}, G. Mantovani^{a,b}, V. Mariani^{a,b}, M. Menichelli^a, A. Saha^a, A. Santocchia^{a,b}, D. Spiga

INFN Sezione di Pisa ^a, Università di Pisa ^b, Scuola Normale Superiore di Pisa ^c, Pisa, Italy

K. Androsov^a, P. Azzurri^{a,15}, G. Bagliesi^a, J. Bernardini^a, T. Boccali^a, L. Borrello, R. Castaldi^a, M.A. Ciocci^{a,b}, R. Dell'Orso^a, G. Fedi^a, L. Giannini^{a,c}, A. Giassi^a, M.T. Grippo^{a,29}, F. Ligabue^{a,c}, T. Lomtadze^a, E. Manca^{a,c}, G. Mandorli^{a,c}, L. Martini^{a,b}, A. Messineo^{a,b}, F. Palla^a, A. Rizzi^{a,b}, A. Savoy-Navarro^{a,31}, P. Spagnolo^a, R. Tenchini^a, G. Tonelli^{a,b}, A. Venturi^a, P.G. Verdini^a

INFN Sezione di Roma ^a, Sapienza Università di Roma ^b, Rome, Italy

L. Barone^{a,b}, F. Cavallari^a, M. Cipriani^{a,b}, D. Del Re^{a,b,15}, M. Diemoz^a, S. Gelli^{a,b}, E. Longo^{a,b}, F. Margaroli^{a,b}, B. Marzocchi^{a,b}, P. Meridiani^a, G. Organtini^{a,b}, R. Paramatti^{a,b}, F. Preiato^{a,b}, S. Rahatlou^{a,b}, C. Rovelli^a, F. Santanastasio^{a,b}

INFN Sezione di Torino ^a, Università di Torino ^b, Torino, Italy, Università del Piemonte Orientale ^c, Novara, Italy

N. Amapane^{a,b}, R. Arcidiacono^{a,c,15}, S. Argiro^{a,b}, M. Arneodo^{a,c}, N. Bartosik^a, R. Bellan^{a,b}, C. Biino^a, N. Cartiglia^a, F. Cenna^{a,b}, M. Costa^{a,b}, R. Covarelli^{a,b}, A. Degano^{a,b}, N. Demaria^a, B. Kiani^{a,b}, C. Mariotti^a, S. Maselli^a, E. Migliore^{a,b}, V. Monaco^{a,b}, E. Monteil^{a,b}, M. Monteno^a, M.M. Obertino^{a,b}, L. Pacher^{a,b}, N. Pastrone^a, M. Pelliccioni^a, G.L. Pinna Angioni^{a,b}, F. Ravera^{a,b}

A. Romero^{a,b}, M. Ruspa^{a,c}, R. Sacchi^{a,b}, K. Shchelina^{a,b}, V. Sola^a, A. Solano^{a,b}, A. Staiano^a, P. Traczyk^{a,b}

INFN Sezione di Trieste ^a, Università di Trieste ^b, Trieste, Italy

S. Belforte^a, M. Casarsa^a, F. Cossutti^a, G. Della Ricca^{a,b}, A. Zanetti^a

Kyungpook National University, Daegu, Korea

D.H. Kim, G.N. Kim, M.S. Kim, J. Lee, S. Lee, S.W. Lee, Y.D. Oh, S. Sekmen, D.C. Son, Y.C. Yang

Chonbuk National University, Jeonju, Korea

A. Lee

Chonnam National University, Institute for Universe and Elementary Particles, Kwangju, Korea

H. Kim, D.H. Moon, G. Oh

Hanyang University, Seoul, Korea

J.A. Brochero Cifuentes, J. Goh, T.J. Kim

Korea University, Seoul, Korea

S. Cho, S. Choi, Y. Go, D. Gyun, S. Ha, B. Hong, Y. Jo, Y. Kim, K. Lee, K.S. Lee, S. Lee, J. Lim, S.K. Park, Y. Roh

Seoul National University, Seoul, Korea

J. Almond, J. Kim, J.S. Kim, H. Lee, K. Lee, K. Nam, S.B. Oh, B.C. Radburn-Smith, S.h. Seo, U.K. Yang, H.D. Yoo, G.B. Yu

University of Seoul, Seoul, Korea

M. Choi, H. Kim, J.H. Kim, J.S.H. Lee, I.C. Park, G. Ryu

Sungkyunkwan University, Suwon, Korea

Y. Choi, C. Hwang, J. Lee, I. Yu

Vilnius University, Vilnius, Lithuania

V. Dudenas, A. Juodagalvis, J. Vaitkus

National Centre for Particle Physics, Universiti Malaya, Kuala Lumpur, Malaysia

I. Ahmed, Z.A. Ibrahim, M.A.B. Md Ali³², F. Mohamad Idris³³, W.A.T. Wan Abdullah, M.N. Yusli, Z. Zolkapli

Centro de Investigacion y de Estudios Avanzados del IPN, Mexico City, Mexico

H. Castilla-Valdez, E. De La Cruz-Burelo, I. Heredia-De La Cruz³⁴, R. Lopez-Fernandez, J. Mejia Guisao, A. Sanchez-Hernandez

Universidad Iberoamericana, Mexico City, Mexico

S. Carrillo Moreno, C. Oropeza Barrera, F. Vazquez Valencia

Benemerita Universidad Autonoma de Puebla, Puebla, Mexico

I. Pedraza, H.A. Salazar Ibarguen, C. Uribe Estrada

Universidad Autónoma de San Luis Potosí, San Luis Potosí, Mexico

A. Morelos Pineda

University of Auckland, Auckland, New Zealand

D. Krofcheck

University of Canterbury, Christchurch, New Zealand

P.H. Butler

National Centre for Physics, Quaid-I-Azam University, Islamabad, Pakistan

A. Ahmad, M. Ahmad, Q. Hassan, H.R. Hoorani, A. Saddique, M.A. Shah, M. Shoaib, M. Waqas

National Centre for Nuclear Research, Swierk, Poland

H. Bialkowska, M. Bluj, B. Boimska, T. Frueboes, M. Górski, M. Kazana, K. Nawrocki, K. Romanowska-Rybinska, M. Szleper, P. Zalewski

Institute of Experimental Physics, Faculty of Physics, University of Warsaw, Warsaw, Poland

K. Bunkowski, A. Byszuk³⁵, K. Doroba, A. Kalinowski, M. Konecki, J. Krolikowski, M. Misiura, M. Olszewski, A. Pyskir, M. Walczak

Laboratório de Instrumentação e Física Experimental de Partículas, Lisboa, Portugal

P. Bargassa, C. Beirão Da Cruz E Silva, B. Calpas, A. Di Francesco, P. Faccioli, M. Gallinaro, J. Hollar, N. Leonardo, L. Lloret Iglesias, M.V. Nemallapudi, J. Seixas, O. Toldaiev, D. Vadrucchio, J. Varela

Joint Institute for Nuclear Research, Dubna, Russia

S. Afanasiev, P. Bunin, M. Gavrilenko, I. Golutvin, I. Gorbunov, A. Kamenev, V. Karjavin, A. Lanev, A. Malakhov, V. Matveev^{36,37}, V. Palichik, V. Perelygin, S. Shmatov, S. Shulha, N. Skatchkov, V. Smirnov, N. Voytishin, A. Zarubin

Petersburg Nuclear Physics Institute, Gatchina (St. Petersburg), Russia

Y. Ivanov, V. Kim³⁸, E. Kuznetsova³⁹, P. Levchenko, V. Murzin, V. Oreshkin, I. Smirnov, V. Sulimov, L. Uvarov, S. Vavilov, A. Vorobyev

Institute for Nuclear Research, Moscow, Russia

Yu. Andreev, A. Dermenev, S. Gninenko, N. Golubev, A. Karneyeu, M. Kirsanov, N. Krasnikov, A. Pashenkov, D. Tlisov, A. Toropin

Institute for Theoretical and Experimental Physics, Moscow, Russia

V. Epshteyn, V. Gavrillov, N. Lychkovskaya, V. Popov, I. Pozdnyakov, G. Safronov, A. Spiridonov, A. Steppenov, M. Toms, E. Vlasov, A. Zhokin

Moscow Institute of Physics and Technology, Moscow, Russia

T. Aushev, A. Bylinkin³⁷

National Research Nuclear University 'Moscow Engineering Physics Institute' (MEPhI), Moscow, Russia

R. Chistov⁴⁰, M. Danilov⁴⁰, P. Parygin, D. Philippov, S. Polikarpov, E. Tarkovskii

P.N. Lebedev Physical Institute, Moscow, Russia

V. Andreev, M. Azarkin³⁷, I. Dremin³⁷, M. Kirakosyan³⁷, A. Terkulov

Skobeltsyn Institute of Nuclear Physics, Lomonosov Moscow State University, Moscow, Russia

A. Baskakov, A. Belyaev, E. Boos, V. Bunichev, M. Dubinin⁴¹, L. Dudko, A. Ershov, A. Gribushin, V. Klyukhin, O. Kodolova, I. Lokhtin, I. Miagkov, S. Obraztsov, M. Perfilov, V. Savrin

Novosibirsk State University (NSU), Novosibirsk, Russia

V. Blinov⁴², Y. Skovpen⁴², D. Shtol⁴²

State Research Center of Russian Federation, Institute for High Energy Physics, Protvino, Russia

I. Azhgirey, I. Bayshev, S. Bitioukov, D. Elumakhov, V. Kachanov, A. Kalinin, D. Konstantinov, V. Krychkine, V. Petrov, R. Ryutin, A. Sobol, S. Troshin, N. Tyurin, A. Uzunian, A. Volkov

University of Belgrade, Faculty of Physics and Vinca Institute of Nuclear Sciences, Belgrade, Serbia

P. Adzic⁴³, P. Cirkovic, D. Devetak, M. Dordevic, J. Milosevic, V. Rekovic

Centro de Investigaciones Energéticas Medioambientales y Tecnológicas (CIEMAT), Madrid, Spain

J. Alcaraz Maestre, M. Barrio Luna, M. Cerrada, N. Colino, B. De La Cruz, A. Delgado Peris, A. Escalante Del Valle, C. Fernandez Bedoya, J.P. Fernández Ramos, J. Flix, M.C. Fouz, P. Garcia-Abia, O. Gonzalez Lopez, S. Goy Lopez, J.M. Hernandez, M.I. Josa, A. Pérez-Calero Yzquierdo, J. Puerta Pelayo, A. Quintario Olmeda, I. Redondo, L. Romero, M.S. Soares, A. Álvarez Fernández

Universidad Autónoma de Madrid, Madrid, Spain

J.F. de Trocóniz, M. Missiroli, D. Moran

Universidad de Oviedo, Oviedo, Spain

J. Cuevas, C. Erice, J. Fernandez Menendez, I. Gonzalez Caballero, J.R. González Fernández, E. Palencia Cortezon, S. Sanchez Cruz, I. Suárez Andrés, P. Vischia, J.M. Vizán Garcia

Instituto de Física de Cantabria (IFCA), CSIC-Universidad de Cantabria, Santander, Spain

I.J. Cabrillo, A. Calderon, B. Chazin Quero, E. Curras, M. Fernandez, J. Garcia-Ferrero, G. Gomez, A. Lopez Virto, J. Marco, C. Martinez Rivero, P. Martinez Ruiz del Arbol, F. Matorras, J. Piedra Gomez, T. Rodrigo, A. Ruiz-Jimeno, L. Scodellaro, N. Trevisani, I. Vila, R. Vilar Cortabitarte

CERN, European Organization for Nuclear Research, Geneva, Switzerland

D. Abbaneo, E. Auffray, P. Baillon, A.H. Ball, D. Barney, M. Bianco, P. Bloch, A. Bocci, C. Botta, T. Camporesi, R. Castello, M. Cepeda, G. Cerminara, E. Chapon, Y. Chen, D. d'Enterria, A. Dabrowski, V. Daponte, A. David, M. De Gruttola, A. De Roeck, E. Di Marco⁴⁴, M. Dobson, B. Dorney, T. du Pree, M. Dünser, N. Dupont, A. Elliott-Peisert, P. Everaerts, G. Franzoni, J. Fulcher, W. Funk, D. Gigi, K. Gill, F. Glege, D. Gulhan, S. Gundacker, M. Guthoff, P. Harris, J. Hegeman, V. Innocente, P. Janot, O. Karacheban¹⁸, J. Kieseler, H. Kirschenmann, V. Knünz, A. Kornmayer¹⁵, M.J. Kortelainen, C. Lange, P. Lecoq, C. Lourenço, M.T. Lucchini, L. Malgeri, M. Mannelli, A. Martelli, F. Meijers, J.A. Merlin, S. Mersi, E. Meschi, P. Milenovic⁴⁵, F. Moortgat, M. Mulders, H. Neugebauer, S. Orfanelli, L. Orsini, L. Pape, E. Perez, M. Peruzzi, A. Petrilli, G. Petrucciani, A. Pfeiffer, M. Pierini, A. Racz, T. Reis, G. Rolandi⁴⁶, M. Rovere, H. Sakulin, C. Schäfer, C. Schwick, M. Seidel, M. Selvaggi, A. Sharma, P. Silva, P. Sphicas⁴⁷, J. Steggemann, M. Stoye, M. Tosi, D. Treille, A. Triossi, A. Tsirou, V. Veckalns⁴⁸, G.I. Veres²⁰, M. Verweij, N. Wardle, W.D. Zeuner

Paul Scherrer Institut, Villigen, Switzerland

W. Bertl[†], K. Deiters, W. Erdmann, R. Horisberger, Q. Ingram, H.C. Kaestli, D. Kotlinski, U. Langenegger, T. Rohe, S.A. Wiederkehr

Institute for Particle Physics, ETH Zurich, Zurich, Switzerland

F. Bachmair, L. Bäni, P. Berger, L. Bianchini, B. Casal, G. Dissertori, M. Dittmar, M. Donegà, C. Grab, C. Heidegger, D. Hits, J. Hoss, G. Kasieczka, T. Klijnsma, W. Lustermann, B. Mangano, M. Marionneau, M.T. Meinhard, D. Meister, F. Micheli, P. Musella, F. Nessi-Tedaldi, F. Pandolfi, J. Pata, F. Pauss, G. Perrin, L. Perrozzi, M. Quittnat, M. Rossini, M. Schönenberger, L. Shchutska, A. Starodumov⁴⁹, V.R. Tavolaro, K. Theofilatos, M.L. Vesterbacka Olsson, R. Wallny, A. Zagozdzińska³⁵, D.H. Zhu

Universität Zürich, Zurich, Switzerland

T.K. Aarrestad, C. Amsler⁵⁰, L. Caminada, M.F. Canelli, A. De Cosa, S. Donato, C. Galloni, A. Hinzmann, T. Hreus, B. Kilminster, J. Ngadiuba, D. Pinna, G. Rauco, P. Robmann, D. Salerno, C. Seitz, A. Zucchetta

National Central University, Chung-Li, Taiwan

V. Candelise, T.H. Doan, Sh. Jain, R. Khurana, M. Konyushikhin, C.M. Kuo, W. Lin, A. Pozdnyakov, S.S. Yu

National Taiwan University (NTU), Taipei, Taiwan

Arun Kumar, P. Chang, Y. Chao, K.F. Chen, P.H. Chen, F. Fiori, W.-S. Hou, Y. Hsiung, Y.F. Liu, R.-S. Lu, M. Miñano Moya, E. Paganis, A. Psallidas, J.f. Tsai

Chulalongkorn University, Faculty of Science, Department of Physics, Bangkok, Thailand

B. Asavapibhop, K. Kovitangoon, G. Singh, N. Srimanobhas

ukurova University, Physics Department, Science and Art Faculty, Adana, Turkey

A. Adiguzel⁵¹, F. Boran, S. Damarseckin, Z.S. Demiroglu, C. Dozen, E. Eskut, S. Girgis, G. Gokbulut, Y. Guler, I. Hos⁵², E.E. Kangal⁵³, O. Kara, A. Kayis Topaksu, U. Kiminsu, M. Oglakci, G. Onengut⁵⁴, K. Ozdemir⁵⁵, S. Ozturk⁵⁶, A. Polatoz, B. Tali⁵⁷, S. Turkcapar, I.S. Zorbakir, C. Zorbilmez

Middle East Technical University, Physics Department, Ankara, Turkey

B. Bilin, G. Karapinar⁵⁸, K. Ocalan⁵⁹, M. Yalvac, M. Zeyrek

Bogazici University, Istanbul, Turkey

E. Gülmez, M. Kaya⁶⁰, O. Kaya⁶¹, S. Tekten, E.A. Yetkin⁶²

Istanbul Technical University, Istanbul, Turkey

M.N. Agaras, S. Atay, A. Cakir, K. Cankocak

Institute for Scintillation Materials of National Academy of Science of Ukraine, Kharkov, Ukraine

B. Grynyov

National Scientific Center, Kharkov Institute of Physics and Technology, Kharkov, Ukraine

L. Levchuk, P. Sorokin

University of Bristol, Bristol, United Kingdom

R. Aggleton, F. Ball, L. Beck, J.J. Brooke, D. Burns, E. Clement, D. Cussans, H. Flacher, J. Goldstein, M. Grimes, G.P. Heath, H.F. Heath, J. Jacob, L. Kreczko, C. Lucas, D.M. Newbold⁶³, S. Paramesvaran, A. Poll, T. Sakuma, S. Seif El Nasr-storey, D. Smith, V.J. Smith

Rutherford Appleton Laboratory, Didcot, United Kingdom

K.W. Bell, A. Belyaev⁶⁴, C. Brew, R.M. Brown, L. Calligaris, D. Cieri, D.J.A. Cockerill, J.A. Coughlan, K. Harder, S. Harper, E. Olaiya, D. Petyt, C.H. Shepherd-Themistocleous, A. Thea, I.R. Tomalin, T. Williams

Imperial College, London, United Kingdom

M. Baber, R. Bainbridge, S. Breeze, O. Buchmuller, A. Bundock, S. Casasso, M. Citron, D. Colling, L. Corpe, P. Dauncey, G. Davies, A. De Wit, M. Della Negra, R. Di Maria, P. Dunne, A. Elwood, D. Futyan, Y. Haddad, G. Hall, G. Iles, T. James, R. Lane, C. Laner, L. Lyons, A.-M. Magnan, S. Malik, L. Mastrolorenzo, T. Matsushita, J. Nash, A. Nikitenko⁴⁹, J. Pela, M. Pesaresi, D.M. Raymond, A. Richards, A. Rose, E. Scott, C. Seez, A. Shtipliyski, S. Summers, A. Tapper, K. Uchida, M. Vazquez Acosta⁶⁵, T. Virdee¹⁵, D. Winterbottom, J. Wright, S.C. Zenz

Brunel University, Uxbridge, United Kingdom

J.E. Cole, P.R. Hobson, A. Khan, P. Kyberd, I.D. Reid, P. Symonds, L. Teodorescu, M. Turner

Baylor University, Waco, USA

A. Borzou, K. Call, J. Dittmann, K. Hatakeyama, H. Liu, N. Pastika

Catholic University of America, Washington DC, USA

R. Bartek, A. Dominguez

The University of Alabama, Tuscaloosa, USA

A. Buccilli, S.I. Cooper, C. Henderson, P. Rumerio, C. West

Boston University, Boston, USA

D. Arcaro, A. Avetisyan, T. Bose, D. Gastler, D. Rankin, C. Richardson, J. Rohlf, L. Sulak, D. Zou

Brown University, Providence, USA

G. Benelli, D. Cutts, A. Garabedian, J. Hakala, U. Heintz, J.M. Hogan, K.H.M. Kwok, E. Laird, G. Landsberg, Z. Mao, M. Narain, S. Piperov, S. Sagir, R. Syarif, D. Yu

University of California, Davis, Davis, USA

R. Band, C. Brainerd, D. Burns, M. Calderon De La Barca Sanchez, M. Chertok, J. Conway, R. Conway, P.T. Cox, R. Erbacher, C. Flores, G. Funk, M. Gardner, W. Ko, R. Lander, C. Mclean, M. Mulhearn, D. Pellett, J. Pilot, S. Shalhout, M. Shi, J. Smith, M. Squires, D. Stolp, K. Tos, M. Tripathi, Z. Wang

University of California, Los Angeles, USA

M. Bachtis, C. Bravo, R. Cousins, A. Dasgupta, A. Florent, J. Hauser, M. Ignatenko, N. Mccoll, D. Saltzberg, C. Schnaible, V. Valuev

University of California, Riverside, Riverside, USA

E. Bouvier, K. Burt, R. Clare, J. Ellison, J.W. Gary, S.M.A. Ghiasi Shirazi, G. Hanson, J. Heilman, P. Jandir, E. Kennedy, F. Lacroix, O.R. Long, M. Olmedo Negrete, M.I. Paneva, A. Shrinivas, W. Si, H. Wei, S. Wimpenny, B. R. Yates

University of California, San Diego, La Jolla, USA

J.G. Branson, S. Cittolin, M. Derdzinski, B. Hashemi, A. Holzner, D. Klein, G. Kole, V. Krutelyov, J. Letts, I. Macneill, M. Masciovecchio, D. Olivito, S. Padhi, M. Pieri, M. Sani, V. Sharma, S. Simon, M. Tadel, A. Vartak, S. Wasserbaech⁶⁶, J. Wood, F. Würthwein, A. Yagil, G. Zevi Della Porta

University of California, Santa Barbara - Department of Physics, Santa Barbara, USA

N. Amin, R. Bhandari, J. Bradmiller-Feld, C. Campagnari, A. Dishaw, V. Dutta, M. Franco Sevilla, C. George, F. Golf, L. Gouskos, J. Gran, R. Heller, J. Incandela, S.D. Mullin, A. Ovcharova, H. Qu, J. Richman, D. Stuart, I. Suarez, J. Yoo

California Institute of Technology, Pasadena, USA

D. Anderson, J. Bendavid, A. Bornheim, J.M. Lawhorn, H.B. Newman, T. Nguyen, C. Pena, M. Spiropulu, J.R. Vlimant, S. Xie, Z. Zhang, R.Y. Zhu

Carnegie Mellon University, Pittsburgh, USA

M.B. Andrews, T. Ferguson, T. Mudholkar, M. Paulini, J. Russ, M. Sun, H. Vogel, I. Vorobiev, M. Weinberg

University of Colorado Boulder, Boulder, USA

J.P. Cumalat, W.T. Ford, F. Jensen, A. Johnson, M. Krohn, S. Leontsinis, T. Mulholland, K. Stenson, S.R. Wagner

Cornell University, Ithaca, USA

J. Alexander, J. Chaves, J. Chu, S. Dittmer, K. McDermott, N. Mirman, J.R. Patterson, A. Rinkevicius, A. Ryd, L. Skinnari, L. Soffi, S.M. Tan, Z. Tao, J. Thom, J. Tucker, P. Wittich, M. Zientek

Fermi National Accelerator Laboratory, Batavia, USA

S. Abdullin, M. Albrow, G. Apollinari, A. Apresyan, A. Apyan, S. Banerjee, L.A.T. Bauerdick, A. Beretvas, J. Berryhill, P.C. Bhat, G. Bolla, K. Burkett, J.N. Butler, A. Canepa, G.B. Cerati, H.W.K. Cheung, F. Chlebana, M. Cremonesi, J. Duarte, V.D. Elvira, J. Freeman, Z. Gecse, E. Gottschalk, L. Gray, D. Green, S. Grünendahl, O. Gutsche, R.M. Harris, S. Hasegawa, J. Hirschauer, Z. Hu, B. Jayatilaka, S. Jindariani, M. Johnson, U. Joshi, B. Klima, B. Kreis, S. Lammel, D. Lincoln, R. Lipton, M. Liu, T. Liu, R. Lopes De Sá, J. Lykken, K. Maeshima, N. Magini, J.M. Marraffino, S. Maruyama, D. Mason, P. McBride, P. Merkel, S. Mrenna, S. Nahn, V. O'Dell, K. Pedro, O. Prokofyev, G. Rakness, L. Ristori, B. Schneider, E. Sexton-Kennedy, A. Soha, W.J. Spalding, L. Spiegel, S. Stoynev, J. Strait, N. Strobbe, L. Taylor, S. Tkaczyk, N.V. Tran, L. Uplegger, E.W. Vaandering, C. Vernieri, M. Verzocchi, R. Vidal, M. Wang, H.A. Weber, A. Whitbeck

University of Florida, Gainesville, USA

D. Acosta, P. Avery, P. Bortignon, A. Brinkerhoff, A. Carnes, M. Carver, D. Curry, S. Das, R.D. Field, I.K. Furic, J. Konigsberg, A. Korytov, K. Kotov, P. Ma, K. Matchev, H. Mei, G. Mitselmakher, D. Rank, D. Sperka, N. Terentyev, L. Thomas, J. Wang, S. Wang, J. Yelton

Florida International University, Miami, USA

Y.R. Joshi, S. Linn, P. Markowitz, G. Martinez, J.L. Rodriguez

Florida State University, Tallahassee, USA

A. Ackert, T. Adams, A. Askew, S. Hagopian, V. Hagopian, K.F. Johnson, T. Kolberg, T. Perry, H. Prosper, A. Santra, R. Yohay

Florida Institute of Technology, Melbourne, USA

M.M. Baarmand, V. Bhopatkar, S. Colafranceschi, M. Hohmann, D. Noonan, T. Roy, F. Yumiceva

University of Illinois at Chicago (UIC), Chicago, USA

M.R. Adams, L. Apanasevich, D. Berry, R.R. Betts, R. Cavanaugh, X. Chen, O. Evdokimov, C.E. Gerber, D.A. Hangal, D.J. Hofman, K. Jung, J. Kamin, I.D. Sandoval Gonzalez, M.B. Tonjes, H. Trauger, N. Varelas, H. Wang, Z. Wu, J. Zhang

The University of Iowa, Iowa City, USA

B. Bilki⁶⁷, W. Clarida, K. Dilsiz⁶⁸, S. Durgut, R.P. Gandrajula, M. Haytmyradov, V. Khristenko, J.-P. Merlo, H. Mermerkaya⁶⁹, A. Mestvirishvili, A. Moeller, J. Nachtman, H. Ogul⁷⁰, Y. Onel, F. Ozok⁷¹, A. Penzo, C. Snyder, E. Tiras, J. Wetzel, K. Yi

Johns Hopkins University, Baltimore, USA

B. Blumenfeld, A. Cocoros, N. Eminizer, D. Fehling, L. Feng, A.V. Gritsan, P. Maksimovic, J. Roskes, U. Sarica, M. Swartz, M. Xiao, C. You

The University of Kansas, Lawrence, USA

A. Al-bataineh, P. Baringer, A. Bean, S. Boren, J. Bowen, J. Castle, S. Khalil, A. Kropivnitskaya, D. Majumder, W. Mcbrayer, M. Murray, C. Royon, S. Sanders, E. Schmitz, R. Stringer, J.D. Tapia Takaki, Q. Wang

Kansas State University, Manhattan, USA

A. Ivanov, K. Kaadze, Y. Maravin, A. Mohammadi, L.K. Saini, N. Skhirtladze, S. Toda

Lawrence Livermore National Laboratory, Livermore, USA

F. Rebassoo, D. Wright

University of Maryland, College Park, USA

C. Anelli, A. Baden, O. Baron, A. Belloni, B. Calvert, S.C. Eno, C. Ferraioli, N.J. Hadley, S. Jabeen, G.Y. Jeng, R.G. Kellogg, J. Kunkle, A.C. Mignerey, F. Ricci-Tam, Y.H. Shin, A. Skuja, S.C. Tonwar

Massachusetts Institute of Technology, Cambridge, USA

D. Abercrombie, B. Allen, V. Azzolini, R. Barbieri, A. Baty, R. Bi, S. Brandt, W. Busza, I.A. Cali, M. D'Alfonso, Z. Demiragli, G. Gomez Ceballos, M. Goncharov, D. Hsu, Y. Iiyama, G.M. Innocenti, M. Klute, D. Kovalskyi, Y.S. Lai, Y.-J. Lee, A. Levin, P.D. Luckey, B. Maier, A.C. Marini, C. Mcginn, C. Mironov, S. Narayanan, X. Niu, C. Paus, C. Roland, G. Roland, J. Salfeld-Nebgen, G.S.F. Stephans, K. Tatar, D. Velicanu, J. Wang, T.W. Wang, B. Wyslouch

University of Minnesota, Minneapolis, USA

A.C. Benvenuti, R.M. Chatterjee, A. Evans, P. Hansen, S. Kalafut, Y. Kubota, Z. Lesko, J. Mans, S. Nourbakhsh, N. Ruckstuhl, R. Rusack, J. Turkewitz

University of Mississippi, Oxford, USA

J.G. Acosta, S. Oliveros

University of Nebraska-Lincoln, Lincoln, USA

E. Avdeeva, K. Bloom, D.R. Claes, C. Fangmeier, R. Gonzalez Suarez, R. Kamalieddin, I. Kravchenko, J. Monroy, J.E. Siado, G.R. Snow, B. Stieger

State University of New York at Buffalo, Buffalo, USA

M. Alyari, J. Dolen, A. Godshalk, C. Harrington, I. Iashvili, D. Nguyen, A. Parker, S. Rappoccio, B. Roozbahani

Northeastern University, Boston, USA

G. Alverson, E. Barberis, A. Hortiangtham, A. Massironi, D.M. Morse, D. Nash, T. Orimoto, R. Teixeira De Lima, D. Trocino, R.-J. Wang, D. Wood

Northwestern University, Evanston, USA

S. Bhattacharya, O. Charaf, K.A. Hahn, N. Mucia, N. Odell, B. Pollack, M.H. Schmitt, K. Sung, M. Trovato, M. Velasco

University of Notre Dame, Notre Dame, USA

N. Dev, M. Hildreth, K. Hurtado Anampa, C. Jessop, D.J. Karmgard, N. Kellams, K. Lannon, N. Loukas, N. Marinelli, F. Meng, C. Mueller, Y. Musienko³⁶, M. Planer, A. Reinsvold, R. Ruchti, G. Smith, S. Taroni, M. Wayne, M. Wolf, A. Woodard

The Ohio State University, Columbus, USA

J. Alimena, L. Antonelli, B. Bylsma, L.S. Durkin, S. Flowers, B. Francis, A. Hart, C. Hill, W. Ji, B. Liu, W. Luo, D. Puigh, B.L. Winer, H.W. Wulsin

Princeton University, Princeton, USA

A. Benaglia, S. Cooperstein, O. Driga, P. Elmer, J. Hardenbrook, P. Hebda, D. Lange, J. Luo, D. Marlow, K. Mei, I. Ojalvo, J. Olsen, C. Palmer, P. Piroué, D. Stickland, A. Svyatkovskiy, C. Tully

University of Puerto Rico, Mayaguez, USA

S. Malik, S. Norberg

Purdue University, West Lafayette, USA

A. Barker, V.E. Barnes, S. Folgueras, L. Gutay, M.K. Jha, M. Jones, A.W. Jung, A. Khatiwada, D.H. Miller, N. Neumeister, J.F. Schulte, J. Sun, F. Wang, W. Xie

Purdue University Northwest, Hammond, USA

T. Cheng, N. Parashar, J. Stupak

Rice University, Houston, USA

A. Adair, B. Akgun, Z. Chen, K.M. Ecklund, F.J.M. Geurts, M. Guilbaud, W. Li, B. Michlin, M. Northup, B.P. Padley, J. Roberts, J. Rorie, Z. Tu, J. Zabel

University of Rochester, Rochester, USA

A. Bodek, P. de Barbaro, R. Demina, Y.t. Duh, T. Ferbel, M. Galanti, A. Garcia-Bellido, J. Han, O. Hindrichs, A. Khukhunaishvili, K.H. Lo, P. Tan, M. Verzetti

The Rockefeller University, New York, USA

R. Ciesielski, K. Goulianos, C. Mesropian

Rutgers, The State University of New Jersey, Piscataway, USA

A. Agapitos, J.P. Chou, Y. Gershtein, T.A. Gómez Espinosa, E. Halkiadakis, M. Heindl, E. Hughes, S. Kaplan, R. Kunnawalkam Elayavalli, S. Kyriacou, A. Lath, R. Montalvo, K. Nash, M. Osherson, H. Saka, S. Salur, S. Schnetzer, D. Sheffield, S. Somalwar, R. Stone, S. Thomas, P. Thomassen, M. Walker

University of Tennessee, Knoxville, USA

M. Foerster, J. Heideman, G. Riley, K. Rose, S. Spanier, K. Thapa

Texas A&M University, College Station, USA

O. Bouhali⁷², A. Castaneda Hernandez⁷², A. Celik, M. Dalchenko, M. De Mattia, A. Delgado, S. Dildick, R. Eusebi, J. Gilmore, T. Huang, T. Kamon⁷³, R. Mueller, Y. Pakhotin, R. Patel, A. Perloff, L. Perniè, D. Rathjens, A. Safonov, A. Tatarinov, K.A. Ulmer

Texas Tech University, Lubbock, USA

N. Akchurin, J. Damgov, F. De Guio, P.R. Duderø, J. Faulkner, E. Gурpinar, S. Kunori, K. Lamichhane, S.W. Lee, T. Libeiro, T. Peltola, S. Undleeb, I. Volobouev, Z. Wang

Vanderbilt University, Nashville, USA

S. Greene, A. Gurrola, R. Janjam, W. Johns, C. Maguire, A. Melo, H. Ni, P. Sheldon, S. Tuo, J. Velkovska, Q. Xu

University of Virginia, Charlottesville, USA

M.W. Arenton, P. Barria, B. Cox, R. Hirosky, A. Ledovskoy, H. Li, C. Neu, T. Sinthuprasith, X. Sun, Y. Wang, E. Wolfe, F. Xia

Wayne State University, Detroit, USA

C. Clarke, R. Harr, P.E. Karchin, J. Sturdy, S. Zaleski

University of Wisconsin - Madison, Madison, WI, USA

J. Buchanan, C. Caillol, S. Dasu, L. Dodd, S. Duric, B. Gomber, M. Grothe, M. Herndon, A. Hervé, U. Hussain, P. Klabbbers, A. Lanaro, A. Levine, K. Long, R. Loveless, G.A. Pierro, G. Polese, T. Ruggles, A. Savin, N. Smith, W.H. Smith, D. Taylor, N. Woods

†: Deceased

- 1: Also at Vienna University of Technology, Vienna, Austria
- 2: Also at State Key Laboratory of Nuclear Physics and Technology, Peking University, Beijing, China
- 3: Also at Universidade Estadual de Campinas, Campinas, Brazil
- 4: Also at Universidade Federal de Pelotas, Pelotas, Brazil
- 5: Also at Université Libre de Bruxelles, Bruxelles, Belgium
- 6: Also at Joint Institute for Nuclear Research, Dubna, Russia
- 7: Also at Helwan University, Cairo, Egypt
- 8: Now at Zewail City of Science and Technology, Zewail, Egypt
- 9: Now at Fayoum University, El-Fayoum, Egypt
- 10: Also at British University in Egypt, Cairo, Egypt
- 11: Now at Ain Shams University, Cairo, Egypt
- 12: Also at Université de Haute Alsace, Mulhouse, France
- 13: Also at Skobeltsyn Institute of Nuclear Physics, Lomonosov Moscow State University, Moscow, Russia
- 14: Also at Ilia State University, Tbilisi, Georgia
- 15: Also at CERN, European Organization for Nuclear Research, Geneva, Switzerland
- 16: Also at RWTH Aachen University, III. Physikalisches Institut A, Aachen, Germany
- 17: Also at University of Hamburg, Hamburg, Germany
- 18: Also at Brandenburg University of Technology, Cottbus, Germany
- 19: Also at Institute of Nuclear Research ATOMKI, Debrecen, Hungary
- 20: Also at MTA-ELTE Lendület CMS Particle and Nuclear Physics Group, Eötvös Loránd University, Budapest, Hungary
- 21: Also at Institute of Physics, University of Debrecen, Debrecen, Hungary
- 22: Also at Indian Institute of Technology Bhubaneswar, Bhubaneswar, India
- 23: Also at Institute of Physics, Bhubaneswar, India
- 24: Also at University of Visva-Bharati, Santiniketan, India
- 25: Also at University of Ruhuna, Matara, Sri Lanka
- 26: Also at Isfahan University of Technology, Isfahan, Iran
- 27: Also at Yazd University, Yazd, Iran
- 28: Also at Plasma Physics Research Center, Science and Research Branch, Islamic Azad University, Tehran, Iran
- 29: Also at Università degli Studi di Siena, Siena, Italy
- 30: Also at INFN Sezione di Milano-Bicocca; Università di Milano-Bicocca, Milano, Italy
- 31: Also at Purdue University, West Lafayette, USA
- 32: Also at International Islamic University of Malaysia, Kuala Lumpur, Malaysia
- 33: Also at Malaysian Nuclear Agency, MOSTI, Kajang, Malaysia
- 34: Also at Consejo Nacional de Ciencia y Tecnología, Mexico city, Mexico
- 35: Also at Warsaw University of Technology, Institute of Electronic Systems, Warsaw, Poland
- 36: Also at Institute for Nuclear Research, Moscow, Russia
- 37: Now at National Research Nuclear University 'Moscow Engineering Physics Institute' (MEPhI), Moscow, Russia
- 38: Also at St. Petersburg State Polytechnical University, St. Petersburg, Russia
- 39: Also at University of Florida, Gainesville, USA
- 40: Also at P.N. Lebedev Physical Institute, Moscow, Russia
- 41: Also at California Institute of Technology, Pasadena, USA
- 42: Also at Budker Institute of Nuclear Physics, Novosibirsk, Russia
- 43: Also at Faculty of Physics, University of Belgrade, Belgrade, Serbia

-
- 44: Also at INFN Sezione di Roma; Sapienza Università di Roma, Rome, Italy
- 45: Also at University of Belgrade, Faculty of Physics and Vinca Institute of Nuclear Sciences, Belgrade, Serbia
- 46: Also at Scuola Normale e Sezione dell'INFN, Pisa, Italy
- 47: Also at National and Kapodistrian University of Athens, Athens, Greece
- 48: Also at Riga Technical University, Riga, Latvia
- 49: Also at Institute for Theoretical and Experimental Physics, Moscow, Russia
- 50: Also at Albert Einstein Center for Fundamental Physics, Bern, Switzerland
- 51: Also at Istanbul University, Faculty of Science, Istanbul, Turkey
- 52: Also at Istanbul Aydin University, Istanbul, Turkey
- 53: Also at Mersin University, Mersin, Turkey
- 54: Also at Cag University, Mersin, Turkey
- 55: Also at Piri Reis University, Istanbul, Turkey
- 56: Also at Gaziosmanpasa University, Tokat, Turkey
- 57: Also at Adiyaman University, Adiyaman, Turkey
- 58: Also at Izmir Institute of Technology, Izmir, Turkey
- 59: Also at Necmettin Erbakan University, Konya, Turkey
- 60: Also at Marmara University, Istanbul, Turkey
- 61: Also at Kafkas University, Kars, Turkey
- 62: Also at Istanbul Bilgi University, Istanbul, Turkey
- 63: Also at Rutherford Appleton Laboratory, Didcot, United Kingdom
- 64: Also at School of Physics and Astronomy, University of Southampton, Southampton, United Kingdom
- 65: Also at Instituto de Astrofísica de Canarias, La Laguna, Spain
- 66: Also at Utah Valley University, Orem, USA
- 67: Also at Beykent University, Istanbul, Turkey
- 68: Also at Bingol University, Bingol, Turkey
- 69: Also at Erzincan University, Erzincan, Turkey
- 70: Also at Sinop University, Sinop, Turkey
- 71: Also at Mimar Sinan University, Istanbul, Istanbul, Turkey
- 72: Also at Texas A&M University at Qatar, Doha, Qatar
- 73: Also at Kyungpook National University, Daegu, Korea